Chapter 4

Preparation of chitosan based nanoparticles for delivery of model drug "venlafaxine hydrochloride"

Contents

4.1 Introduction

Chitin is a fibrillar crystalline polymer of unbranched chain of 2-acetamido- 2-deoxy-(1-4)- β -D-glucopyranose residues (N-acetyl-D-glucosamine units), which belongs to the family of polysaccharides. Insect skins and the shells of anthropoids are composed of chitin. Chitosan (CS), the N-deacetylated derivative of chitin poly (β-(1-4)-2-amino-2-deoxy-D-glucopyranose) obtained by alkaline treatment, is a biocompatible, biodegradable and nontoxic polyelectrolyte. Chitosan chemistry has been widely investigated due to basic scientific interest as well as its use in food industry and in biomedical and agricultural applications. In comparison with the cellulose, chitosan has more reactive centers in its structure, and depending on the reaction conditions, substitution at 0- and/or N can take place. In an acidic medium or without a catalyst, reactions can take place at the nitrogen from -NH_2 group. In an alkaline medium, the alkoholate ion is more reactive and substitution can occur at oxygen. In the last decade, several synthetic as well as natural polymers have been examined for pharmaceutical applications. After cellulose, with which it bears a structural resemblance, chitosan is next abundant natural polymer. Due to its specific structure and properties, chitosan has found a number of applications in drug delivery including as an absorption enhancer for hydrophilic macromolecular drugs and as a gene delivery system[1-8]. The polymer is comprised of copolymers of glucosamine and N-acetyl glucosamine and its molecular formula is $C_6H_{11}O_4N$. The term chitosan holds a series of polymers that vary in molecular weight (from approximately 10,000 to 1 million Dalton) and degree of deacetylation (in the range of 50-95 %). Since chitosan displays mucoadhesive properties, strong permeation enhancing capabilities for hydrophilic compounds and a safe toxicity profile[9-10], it has received considerable attention as a novel excipient in drug delivery system and has been included in the European Pharmacopoeia since 2002. Due to the presence of free hydroxyl and amino groups, it can bind strongly to negatively charged surfaces of cells, mucus or other negatively charged polymers by electrostatic or hydrogen bonding and can also be chemically modified to suit for enzyme immobilization[11], separation media[12], protein

adsorption[13], absorbable sutures[14], food and nutrition[15], photography[16] and in controlled release drug delivery systems in various forms[17-21].

Nanoparticles have increasingly been investigated as carriers for hydrophilic macromolecular moieties such as peptides, proteins, vaccines, drugs and DNA to improve stability and permit administration through non-parenteral routes[22-31]. Although a wide variety of techniques are available for producing nanoparticles including solvent evaporation[32], interfacial polymerization[33] and emulsion polymerization[34], most of these approaches involve use of organic solvents, heating or vigorous agitation, which are potentially harmful to sensitive biomolecules. Hence an alternative route is desired to overcome the above disadvantages. Calvo *et al*[35] prepared chitosan nanoparticles by ionotropic gelation of chitosan with tripolyphosphate (TPP) counterions. Since then, majority of chitosan nanoparticles have been reported to be prepared by this technique. Ionotropic gelation occurs through intermolecular or intramolecular linkages between positively charged quaternary amine groups from chitosan in acidic medium, with negatively charged multivalent counter ion like TPP[36] without using cross linkers. Bodmeier *et al*[37] were the first to report the ionotropic gelation of chitosan with tripolyphosphate for drug encapsulation. Subsequently increase in research in the preparation of CS/TPP nanoparticles for successful delivery of small drugs, proteins and genes is reflected in the increased number of published papers in this field. ***Table 4.1*** gives a brief summary of published research works based on CS/TPP nanoparticles used for encapsulation of various bioactive molecules in last 10 years. It was reported that hydrophilic nanoparticles based on chitosan have received increasing attention due to their ability to cross the biological barrier by protecting the entrapped drug. The applications of chitosan in the biomedical field are limited, due to its poor solubility in physiological media. Chitosan is only soluble in aqueous acidic solutions below pH 6.5, in which the primary amino groups of chitosan get protonated. To improve the poor water-solubility of chitosan, several derivatisations such as quaternization of the amino groups, N-carboxymethylation and PEGylation[38] have been proposed. Hydrophobic character of chitosan can also be altered through blending, grafting and chemical modification using poly(vinyl alcohol), poly(vinyl pyrrolidone) and poly(ethylene glycol) and PEG derivatives[39].

Table 4.1 Summary of works on CS/TPP nanoparticles used for encapsulation of bioactive molecules.

Article Title, Author	Description	Ref
Physicochemical characterization and antioxidant activity of Quercetin-loaded chitosan nanoparticles ***Zhang Y et al 2008***	Nanoparticles were prepared based on the ionic gelation method. AFM, DSC, XRPD, FTIR, UV-Vis, and fluorescence spectrometry were used to characterize the inclusion compounds and their antioxidant activity was evaluated.	40
Chitosan nanoparticles loaded with dorzolamide and pramipexole. ***Papadimitriou S et al. 2008***	An efficient ocular formulation for Dorzo and Prami was prepared by ionic gelation methods. Effect of CS/drug ratio on particle size, drug association efficiency, loading efficiency and release profile was evaluated. Sustained in vitro drug release was observed with both drugs.	41
Cavitation effects versus stretch effects resulted in different size and polydispersity of ionotropic gelation chitosan–sodium tripolyphosphate nanoparticle ***Tsai M L et al 2007***	Effect of different modes of input-energy levels (cavitation effects versus stretch effects) on the size and polydispersity of chitosan–sodium tripolyphosphate (TPP) Nanoparticles was compared. It was reported that the particle size can be manipulated by varying different mechanical energy of ultrasonic radiation or mechanical shearing.	42
Chitosan Nanoparticles for Loading of Toothpaste Actives and Adhesion on Tooth Analogs ***Liu H et al 2007***	Nanoparticles are scarcely applied as delivery vehicle for toothpaste actives. The adhesion, drug loading, and release of the chitosan nanoparticles were studied. The loaded toothpaste actives showed a sustained release behavior for at least 10 h. All the particles could adhere onto the tooth analogs and In vitro cell culture did not find any cytotoxicity.	43
Preparation of Nanoparticles Composed of Chitosan and Its Derivatives as Delivery	Quaternized chitosan (O-HTCC) and its nanoparticles were prepared successfully using a simple and mild ionic-gelation method. These nanoparticles have narrow size distribution and	44

Systems for Macromolecules ***Sun and Wan 2007***	positive surface charges. Bovine serum albumin (BSA), as a model protein drug, was incorporated into the nanoparticles. High BSA loading efficiency (87.5%) and loading capacity (99.5%) are achieved by quaternized chitosan (O-HTCC) nanoparticles, and the release profile of BSA from nanoparticles has an obvious burst effect followed by a slow continuous release.	
Chitosan nanoparticle as protein delivery carrier—Systematic examination of fabrication conditions for efficient loading and release. ***Gan Q and Wang T 2007***	This work seeks to further explore the polyionic coacervation fabrication process, and associated processing conditions under which protein encapsulation and subsequent release can be systematically and predictably manipulated so as to obtain desired effectiveness. BSA was used as a model protein which was encapsulated by either incorporation or incubation method, using the polyanion tripolyphosphate (TPP) as the coacervation crosslink agent.	45
Preparation and Characterization of Nanoparticles Shelled with Chitosan for Oral Insulin Delivery ***Lin Y H et al*** ***2007***	Nanoparticles composed of chitosan and poly (glutamic acid) were prepared by a simple ionic-gelation method for oral insulin delivery. After loading of insulin, the NPs remained spherical and the insulin release profiles were significantly affected by their stability in distinct pH environments. In vivo results clearly indicated that the insulin-loaded NPs could effectively reduce the blood glucose level in a diabetic rat model.	46
Characterization of insulin-loaded alginate nanoparticles produced by ionotropic pre-gelation through DSC and FTIR studies. ***Sarmento B et al 2006***	Insulin-loaded nanoparticles were prepared by ionotropic pre-gelation of alginate with calcium chloride followed by complexation between alginate and chitosan. Individual and smaller sizing nanoparticles, around 800 nm, were obtained at pH 4.7 with an alginate: chitosan mass ratio of 6:1. DSC and FTIR were successfully used to characterize the nanoparticulate systems.	47
Studies on Effect of pH on Cross-linking of Chitosan With Sodium Tripolyphosphate: A Technical Note.	In the present work, systematic study was carried out to gain insight on the mechanistic basis of the ionotropic gelation of chitosan with TPP. With this view, the effect of pH of TPP on chitosan-tripolyphosphate cross-linking was investigated.	48

Bhumkar D R and Pokharkar V B 2006	Chitosan was cross-linked ionically with TPP at lower pH and by deprotonation mechanism at higher pH.	
Preparation and Characterization of Chitosan-Based Nanoparticles. ***Bodnar M et al 2005***	Novel biodegradable nanoparticles based on chitosan with natural di- and tricarboxylic acids were synthesized for biomedical applications. The size of colloid dispersion ranges from 270 to 370 nm. The condensation reaction of carboxylic groups and pendant amino groups of chitosan were performed by using water-soluble carbodiimide. This method allows the formation of polycations, polyanions, and polyampholyte nanoparticles. The prepared nanosystems were stable in aqueous media at low pH, neutral, and mild alkaline conditions.	49
Chitosan nanoparticles as a novel delivery system for ammonium glycyrrhizinate. ***Wu Y et al 2005***	CS nanoparticles had shown an excellent capacity for the association (upto 90%) of ammonium glycyrrhizinate. Effect of solution parameters on size and encapsulation efficiency was studied. Initial burst and a slow release profile was observed.	50
Chitosan drug binding by ionic interaction. ***Boonsongrit Y et al 2005***	Three model drugs (insulin, diclofenac sodium and salicylic acid) with different pKa were used to prepare drug-polymer micro/nanoparticles by ionic intraction. A high entrapment efficiency of the micro/nanoparticles could be obtained by careful control of formulation pH but it has no effect on burst release. Drug with highest ionization range shows lowest entrapment.	51
Microencapsulated chitosan nanoparticles for lung protein delivery. ***Grenha A et al 2005***	Microencapsulated protein loaded CS/TPP nanoparticles were prepared by spray drying technique using typical aerosol excipients, such as mannitol and lactose. These NPs show a good protein loading capacity (65-80%). The particles were mostly spherical and possess appropriate aerodynamic properties for pulmonary delivery.	52
Preparation and in-vitro evaluation of chitosan nanoparticles containing a	Formulation for Z-DEVD-FMK, a peptide which is a caspase inhibitor and has been used in experimental animal studies for a decade was	**53**

caspase inhibitor. ***Aktas Y et al 2005***	prepared from ionic gelation method and quantified by HPLC. The formulation with the initial peptide concentration of 400 ng/mL provided the highest loading capacity (0.46 %) and the highest extent of release (65 % at 24 h).	
Physicochemical characterization of chitosan nanoparticles: electrochemical and stability behavior. ***Lopex-Leon T et al 2005***	This work shows a systematic study on the chemical physical characterization of gel nanoparticles formed by chitosan chains electrostatically linked by ionic interactions. The stability; phase transition and electric states of particles have been extensively analyzed by means of PCS, SLS and electrophoretic mobility measurements.	54
Effect of molecular structure of chitosan on protein delivery properties of chitosan nanoparticles. ***Xu Y and Du Y 2003***	Chitosan nanoparticles with diameter 20- 200 nm and spherical shape were prepared by ionic gelation method. Factors affecting delivery properties of bovine serum albumin (BSA) as model protein have been tested; they included molecular weight (Mw) and deacetylation degree (DD) of chitosan, the concentration of chitosan and initial BSA. Increasing Mws of chitosan from 10 to 210 kDa, BSA encapsulation efficiency was enhanced about two times, BSA total release in PBS (phosphate buffer saline) at pH 7.4 in 8 days was reduced from 73.9 to 17.6%. Increasing DD from 75.5 to 92% promoted slightly the encapsulation efficiency and decelerated the release rate. The encapsulation efficiency decreased with increase in initial BSA and chitosan concentration.	**55**
Nasal delivery of Insulin using Novel Chitosan based formulations: A Comparative study in Two animal Models between simple chitosan formulations and chitosan nanoparticles ***Dyer A M et al 2002***	To investigate weather the widely accepted use of chitosan as a nasal drug delivery system, might be further improved by application of chitosan formulated as nanoparticles prepared by ionic gelation method. It was shown conclusively that chitosan nanoparticles did not improve the absorption enhancing effect of chitosan in solution or powder form and that chitosan powder was the most effective formultion for nasal delivery of insulin in the sheep model.	56

Chitosan nanoparticles as delivery systems for doxorubicin ***Janes K A et al*** ***2001***	To evaluate the potential of CS nanoparticles as carriers for the cationic hydrophilic anthracycline drug molecule formed by ionic gelation of the positively charged CS. Positive charge of drug molecule was masked by complexing with polyanion, dextran sulphate. By these modifications, doubled encapsulation efficiency relative to controls was obtained and enabled real loadings up to 4 wt % and a very slow release.	57
Chitosan and chitosan/ethylene oxide-propylene oxide block copolymer nanoparticles as novel carriers for proteins and vaccines. ***Calvo P et al*** ***1997***	To investigate the interaction between the components of novel CS and CS/PEO-PPO block copolymer Nanoparticles and to evaluate their potential for the association and controlled release of proteins and vaccines. XPS study proved the presence of PEO-PPO on the surface and its interaction with CS. BSA, tetanus and diphtheria toxoids were highly associated with CS Nanoparticles and each protein were released from the NPS at controlled rate and tetanus vaccine was released in the active form for at least 15 days.	58
Novel Hydrophilic Chitosan–Polyethylene Oxide Nanoparticles as Protein Carriers ***Calvo P et al*** ***1997***	A new approach for the preparation of nanoparticles made solely of hydrophilic polymers is presented. The preparation technique, based on an ionic gelation process, is extremely mild. Size (200–1000 nm) and zeta potential (between /20 mV and /60 mV) of nanoparticles can be conveniently modulated by varying the ratio CS/PEO–PPO. Furthermore, using bovine serum albumin (BSA) as a model protein it was shown that these new nanoparticles have a great protein loading capacity (entrapment efficiency up to 80% of the protein) and provide a continuous release of the entrapped protein up to 1 week.	35

Chitosan nanoparticles prepared by different preparation protocols have been widely studied carriers for various pharmaceutically active ingredients with varying degree of effectiveness and drawbacks. In the present work, Ionic complexation process has been further used in the preparation of CS/TPP nanocarriers for the model drug venlafaxine hydrochloride and subsequent study of in-vitro release profiles of venlafaxine hydrochloride from the nanoparticles. Optimization of the experimental conditions was done in order to achieve

maximum encapsulation efficiency and controlled release of venlafaxine hydrochloride from CS/TPP nanoparticles[59].

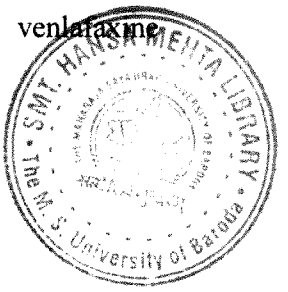

4.2 Experimental

4.2.1 Materials

Venlafaxine hydrochloride was obtained as a gift sample from Alembic Chemicals Ltd (Vadodara, India). Venlaflaxine, is chemically known as (R/S)-1-[2-(dimethylamino)-1-(4-methoxyphenyl) ethyl]-cyclohaxanol and belongs to a class of hydroxyl cycloalkane phenethyl amines. It is used as antidepressants. Venlaflaxine hydrochloride is approved for sale in various countries including U.S. under the brand name EFFEXOR.RTM. (Wyeth Ayerst). Venlafaxine hydrochloride is highly soluble in water. It is well known that it is very difficult to develop a pharmaceutical formulation with a very slow dissolution rate of freely soluble drug.

Chitosan is commercially available through various manufacturers worldwide. Depending on the source and preparation procedure, molecular weight may range from 30-kilo Daltons (KDa) to over 1000 KDa. Commercially available preparations have degrees of deacetylation (DD) ranging from 50 to 98%. A polysaccharide with greater than 50% of the amino groups deacetylated is termed chitosan, and one with less is termed chitin. Many methods have been used to determine the DD of chitosan. These include infrared spectrometry (IR)[60-62], near infrared spectrometry (NIR)[63], UV-spectrophotometry[64], first derivative UV-spectrophotometry (1DUVS)[65], colloidal titration[66], enzymatic determination[67], nuclear magnetic resonance spectrometry (NMR)[68], ninhydrin test[69] and circular dichroism measurements[70]. The choice of method appears to be arbitrary and often does not correlate well with others. A standard method used to determine the DD of chitosan has to be simple, rapid and cost effective. Chitosan derived from crab shell, in the form of fibrilar flakes was obtained from Sigma-Aldrich (Sting-ham, Germany). The degree of deacylation and molecular weight of chitosan were determined from FTIR analysis and viscosity method and were observed to be 87 % and 70 KDa respectively. Sodium tripolyphosphate (TPP) was purchased from Sulab Chemicals (Baroda, India). Polyethylene glycol ($\overline{M}_n$ = 4000 units) and

acetic acid were obtained from Merck, Mumbai, India. All other reagents used were of analytical grade.

4.2.2. A. Preparation of CS/TPP nanoparticles

The hydrophilic nanoparticles were prepared using complex coacervation of chitosan with tripolyphosphate according to the procedure reported by Calvo *et al*[35] based on the ionic gelation of CS with TPP anions. A polycationic polysaccharide CS solution and a solution containing polyanion TPP were mixed at room temperature under magnetic stirring to produce CS/TPP nanoparticles. CS and TPP, when mixed, undergo a coacervation process, as a result of ionotropic interaction between positively charged quaternary amino groups of chitosan with the negatively charged TPP. Although, CS/TPP nanoparticles are formed under mild conditions, nature and extent of ionic interaction were found to be sensitive to variables such as molecular weight, degree of deacylation, molar ratio of CS to TPP, charge density of both electrolytes and blending with other polymer.

Stock solution of chitosan (1 % w/v) was prepared by dissolving 1g of chitosan in 100 mL of 1 % v/v acetic acid under magnetic stirring at room temperature until the solution became transparent. The solution was filtered through 0.2 micron nylon filter before use. Solutions with different concentrations (0.05 % to 0.25 % w/v) of chitosan were prepared from stock solution and used successively for the preparation of nanoparticles. Tripolyphosphate solution of 0.05 % w/v was prepared by dissolving 0.5 g of TPP in 1 liter of distilled deionized water. Addition of variable volumes of TPP solution to 4 ml of the chitosan solution of different concentrations lead into spontaneous formation of CS/TPP nanoparticles at room temperature under magnetic stirring for a period of 30 minutes[59].

4.2.2. B. Preparation of venlafaxine hydrochloride loaded CS/TPP nanoparticles

Incorporation of venlafaxine hydrochloride into the nanoparticles was done by dissolving venlafaxine hydrochloride in either the polycation CS or polyanion TPP. Different concentrations of venlafaxine hydrochloride (0.2, 0.4, 0.6, 0.8, 1.0 mg/mL) were added to chitosan solution (0.15 % w/v) and gently

mixed for 30 minutes under mild magnetic stirring before the addition of TPP solution (0.05 % w/v). The venlafaxine hydrochloride loaded CS/TPP nanoparticles were formed spontaneously upon addition of variable volumes of TPP in 4 mL of CS solution under mild magnetic stirring for 30 minutes at room temperature (30 ± 2 °C)[59].

4.2.2. C. Preparation of venlafaxine hydrochloride loaded PEG coated CS/TPP nanoparticles

Different concentrations of PEG 4000 (10-50 mg/ml) were added to 4mL of 0.15 % w/v chitosan solution containing 600 µg/mL venlafaxine hydrochloride and gently mixing for 30 minutes under mild magnetic stirring before the addition of TPP solution (0.05 % w/v). The PEG coated CS/TPP nanoparticles were formed spontaneously upon addition of variable volumes of TPP and stirring it magnetically for 30 minute at 30 ± 2 °C[59].

4.2.3 Characterization of nanoparticles

CS/TPP nanoparticles were collected by centrifugation at 25,000 rpm for 30 minute at room temperature (30 ± 2 °C). Supernatant solution was discarded and nanoparticles were resuspended in double distilled deionized water and then lyophilized for a period of 24 h to get dry nanoparticles.

4.2.3.a Fourier transform infrared spectrometry (FTIR)

FTIR spectrum of CS, venlafaxine hydrochloride, placebo nanoparticles, venlafaxine hydrochloride loaded CS/TPP nanoparticles and PEG coated CS/TPP nanoparticles were recorded on a Perkin Elmer Rx_I FTIR spectrophotometer (Massachusetts, USA) using 1 cm diameter KBr pellets.

4.2.3.b Differential scanning calorimetry (DSC)

DSC analysis was carried out using a Mettler–Toledo 822 instrument (Greifensee, Switzerland). The instrument was calibrated using indium as a standard and samples (CS, venlafaxine hydrochloride, placebo nanoparticles, venlafaxine hydrochloride loaded CS/TPP nanoparticles and PEG coated CS/TPP

nanoparticles) were heated in sealed aluminum pans between 30 °C to 400 °C at a heating rate of 10 °C min^{-1}.

4.2.3.c Powder X-ray diffraction (XRD)

XRD patterns for CS, PEG, venlafaxine hydrochloride, placebo nanoparticles, venlafaxine hydrochloride loaded CS/TPP nanoparticles and PEG coated CS/TPP nanoparticles were recorded on a Philips X'pert multipurpose diffreactometer (MPD range, Germany) using a Ni-filtered Cu Kα radiation over the 2θ range of 3-100°.

4.2.3.d Transmittance electron microscopy (TEM)

The morphology, size and shape of the placebo nanoparticles, drug loaded CS/TPP nanoparticles and PEG coated CS/TPP nanoparticles were examined by using Transmission electron microscope (Philips CM 120, Eindhoven, Netherlands) at accelerating voltage of 200 KeV. One drop of the prepared CS/TPP nanoparticles suspension was placed on 300 mesh carbon coated copper grid. The grid was dried under IR lamp and the images of representative areas were taken at suitable magnifications.

4.2.3.e Particle size and zeta potential measurement

A Brookhaven's 90 plus dynamic light scattering (Holtsville, USA) equipment with a 15 mW solid state laser source operating at 688 nm was used to measure the particle size and size distribution of freshly prepared CS/TPP nanoparticles and drug loaded CS/TPP nanoparticles in a dynamic mode. The scattering intensities from the samples were measured at 90° using photomultiplier tube. Average hydrodynamic radius of latex particles (R_h) was calculated from the intrinsic diffusion coefficient (Do) as

$$\boxed{R_h = KT / (6 \pi \eta D_0)} \qquad (1)$$

where K is a Boltzmann constant, T is the absolute temperature and η is the viscosity of the dispersing medium. The polydispersity index (PI), which is the variance of the size distribution, was obtained with the PSDW 32 bit software provided with the instrument.

The zeta potential of the nanoparticles was measured using Brookhaven's 90 plus dynamic light scattering instrument. Measurements were carried out at room temperature (30 ± 2 °C). For zeta potential measurements, samples were diluted 10-100 times with 0.1 mM KCl and placed in the electrophoretic cell where a potential of ± 150 mV was applied. All measurements were performed in triplicate. The performance of the zetasizer was checked for its consistency by determining the zeta potential value of a standard colloidal ink solution (ZR3) supplied by the Brookhaven, USA. The samples for calibrating the instrument were prepared in 0.1 mM KCl with appropriate dilution.

4.2.3.f X-ray photoelectron spectrometry (XPS)

XPS analysis was carried out using VG Scientific ESCALAB MK II spectrometer equipped with Al/Mg twin anode. Survey scan and multiscan quantitative data were collected using Aluminium-Pottasium (Al-K) source operated at 50 eV analyzer pass energy and high resolution data was collected using 20 eV pass energy. Vacuum in the analysis chamber was maintained better than 10^{-8} m.Bar throughout XPS experiments. The spectrometer was calibrated using Ag ($3d_{5/2}$) photoelectron line of silver. The C (1S) photoelectron line from neutral carbon at 285 eV was used as internal reference in binding energy measurements. Binding energy measurements were accurate to ± 0.1 eV and are average of two experiments. Data was analyzed on DELL computer interfacing the spectrometer.

4.2.3.g Drug encapsulation efficiency of nanoparticles

The drug encapsulation efficiency was determined by the separation of the nanoparticles from the aqueous medium containing non-associated venlafaxine hydrochloride by centrifugation at 25,000 rpm for 30 minutes at room temperature (30 ± 2 °C). The amount of free drug in supernatant was quantified by measuring absorbance at 274 nm using Perkin Elmer Lambda 35 UV spectrophotometer. The venlafaxine hydrochloride encapsulation efficiency (% EE) of the nanoparticles was calculated according to following equation: All measurements were performed in triplicate.

$$EE = \frac{\text{Total Venlafaxine hydrochloride - Free Venlafaxine hydrochloride}}{\text{Total Venlafaxine hydrochloride}} \quad (2)$$

4.2.3.h In-vitro release

In vitro release study was performed according to the procedure reported by Hu and Lopina[71]. In vitro release of venlafaxine hydrochloride from CS/TPP nanoparticles was studied by redispersing separated nanoparticles (10 mg) in 2.5 mL freshly prepared phosphate buffer of pH 7.4, in a dialysis membrane bag with molecular weight cut off at 5 KDa. The dialysis bag was placed in 50 mL of phosphate buffer of pH 7.4. The entire system was kept under magnetic stirring. 4 mL of the release medium was removed and simultaneously replaced by fresh buffer solution at regular time intervals. The amount of drug in the release medium was evaluated by measuring absorbance at 274 nm. All the release studies were conducted in triplicate.

4.3 Results and Discussion

In the present study we adapted the method of Calvo *et al*[35] for the preparation of nanoparticulate system made of solely hydrophilic polymers. These nanoparticles are composed of cationic and anionic polymers CS and TPP. The preparation technique involves the mixture of two aqueous phases containing CS and TPP stirred under mild condition at room temperature (30 ± 2 °C). Nanoparticles are formed by coacervation, which is a spontaneous phase separation process arising from electrostatic interaction when oppositely charged macromolecules are mixed together. The success of the process is largely dependent on intermolecular linkages created between the negatively charged groups of TPP with that of positively charged amino groups of CS. A Similar principle has been used by other research groups for the preparation of such nanoparticles for the encapsulation and release of genes, proteins, peptides, insulin etc from the nanoparticulate system as described in ***Table 4.1***. The present study, as far as the author is aware, however, is the first attempt reported to use CS/TPP matrix materials for incorporation of venlafaxine hydrochloride into a CS/TPP nanoparticle system. The molecular structures of venlafaxine hydrochloride,

sodium tripolyphosphate and chitosan, are given in ***Figure 4.1***. The advantages of this technique include:

- CS/TPP nanoparticles are prepared under extremely mild conditions and a short reaction time without involving high temperature, sonication or organic solvents.
- Particle size and surface charge can be modulated by varying the ratio of CS/TPP.
- Excellent loading capacity for venlafaxine hydrochloride and also continuous release of drug from the nanoparticulate system for extended period of time can be achieved.
- Presence of PEG on the surface of CS/TPP nanoparticles, a fact that makes them interesting carrier for drug delivery applications.

All these features make this nanoparticulate system a promising carrier for bioactive molecules like venlafaxine hydrochloride.

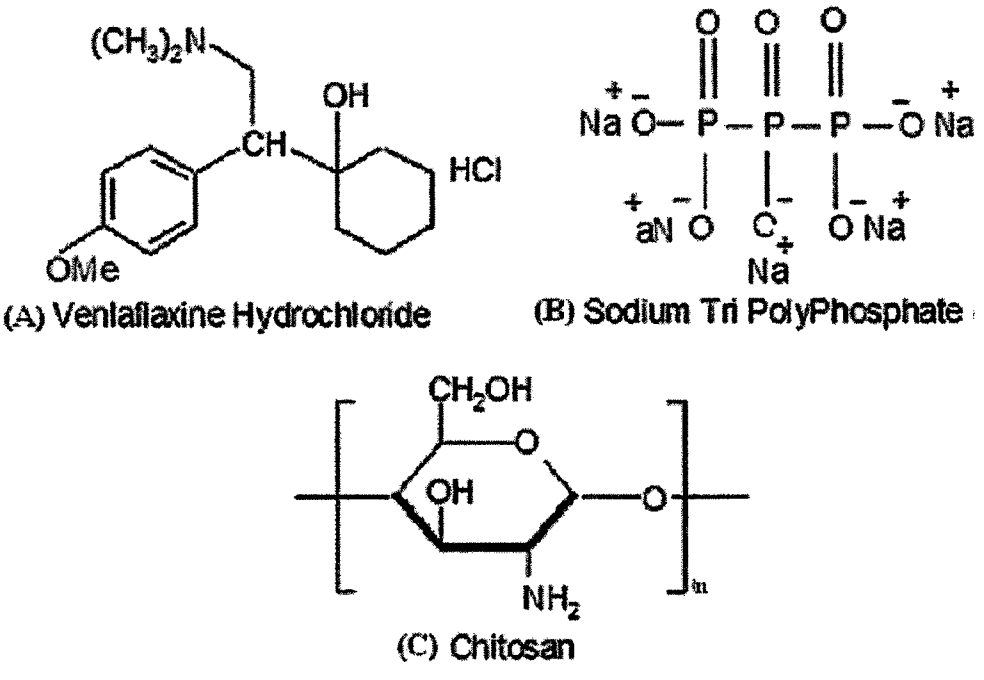

Figure 4.1 Molecular structures of (A) venlafaxine hydrochloride, (B) sodium tripolyphosphate and (C) chitosan.

4.3.1 Optimization of conditions for the formation of CS/TPP nanoparticles

The physicochemical properties of nanoparticles are important in determining the physiological functions and stability of nanoparticles loaded with drugs. The particle size is one of the most significant determinants in mucosal and epithelial tissue uptake and intracellular trafficking[72]. Surface charge is another important determinant in not only the stability, mucoadhesiveness, and permeation enhancing effects of nanoparticles[73, 74] but also the ability of nanoparticles to escape from the endolysosomes[75]. CS/TPP nanoparticles can easily be prepared on mixing of TPP solution with CS solution under stirring, as the formation of nanoparticles is based on an ionic gelation technique between positively charged CS and negatively charged TPP. It is noteworthy that many researchers have explored the capacity of CS/TPP nanoparticles to associate with peptides, proteins, oligonucleotides, and plasmids DNA for potential pharmaceutical applications. As the physicochemical features of CS/TPP nanoparticles may affect the stability, as a result of stable ionic interactions and biological performance of nanoparticles loaded with target molecules, it is important to elucidate the effect of preparation conditions on particle size or stability of CS/TPP nanoparticles. Therefore, we investigated the effects of CS concentration and CS/TPP mass ratio on particle size and surface charge of CS/TPP nanoparticles.

➢ Effect of chitosan concentration

A preliminary screening of different concentration ratios of CS/TPP combinations showed that, mainly both polymer ratio and total polymer concentration influenced the formation of nanoparticles. To examine effect of chitosan concentration on nanoparticles formation, chitosan solutions of different concentrations ranging from 0.05-0.25 % (w/v) in 1 % acetic acid were reacted efficiently with 0.05 % aqueous solution of tripolyphosphate. Concentration of drug was kept constant at already optimized condition of 600 µg/ml and pH of the medium was maintained at 5. The mixture was stirred magnetically for 30 minutes. The nanoparticles were observed to be formed only at CS/TPP mass ratios 5:1. The results of effect of chitosan concentration on particle size and zeta potential at fixed drug concentration (600 µg/ml) are presented in ***Figure 4.2***. All

results are based on triplicate analysis of each sample analyzed through dynamic light scattering technique. The relative standard deviation was observed to be well below 2 % in all cases.

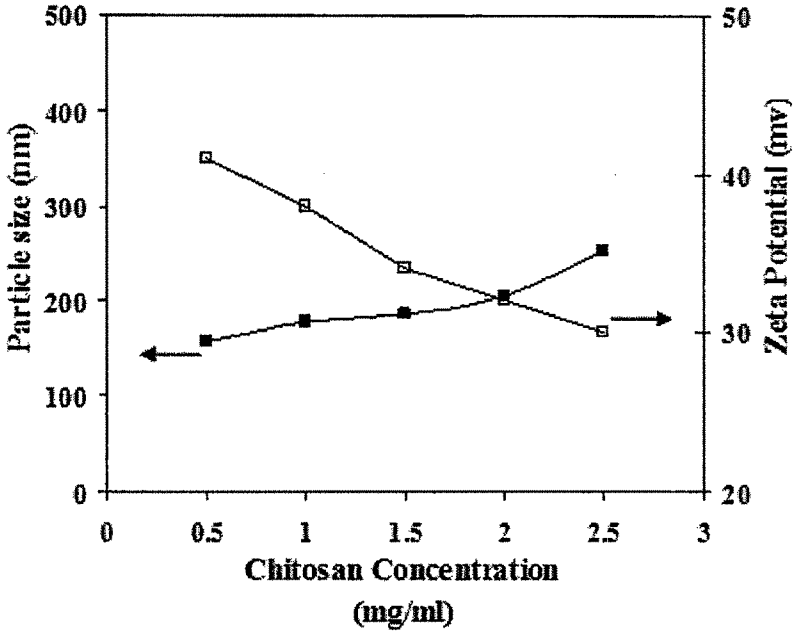

Figure 4.2 Effect of chitosan concentration on (■) particle size and (□) zeta potential at CS/TPP mass ratio 5:1 and pH = 5.

From the nature of the graph it is observed that particle size increases and zeta potential decreases with increasing CS concentration. Similar observation is reported earlier in the literature[76]. This can be attributed to the increased viscosity of chitosan solution with increase in its concentration, which reduces the ionic interaction of CS with TPP leading to increase in particle size.

➢ Effect of CS/TPP mass ratio

CS/TPP mass ratio is another important factor influencing the characteristics of the formed CS/TPP nanoparticles. It was observed that nanoparticles were formed only at specific concentration of CS and CS/TPP mass ratio. To examine the effect of CS/TPP mass ratio on particle size and zeta potential, nanoparticles were prepared as described earlier, at fixed concentration of chitosan (1.5 mg/ml). It was observed that, when the CS/TPP mass ratio was

kept below 3:1, formed CS/TPP nanoparticles suspension become more and more turbid and also opalescent flocculates were observed. A similar phenomenon was reported earlier[55, 79]. ***Figure 4.3*** shows the effect of CS/TPP mass ratio on particle size and zeta potential of CS/TPP nanoparticles. Variation in CS/TPP mass ratio from 3:1 to 7:1 showed increase in particle size as well as zeta potential of nanoparticles. Similar observation is reported earlier in the literature by Hu *et al*[76].

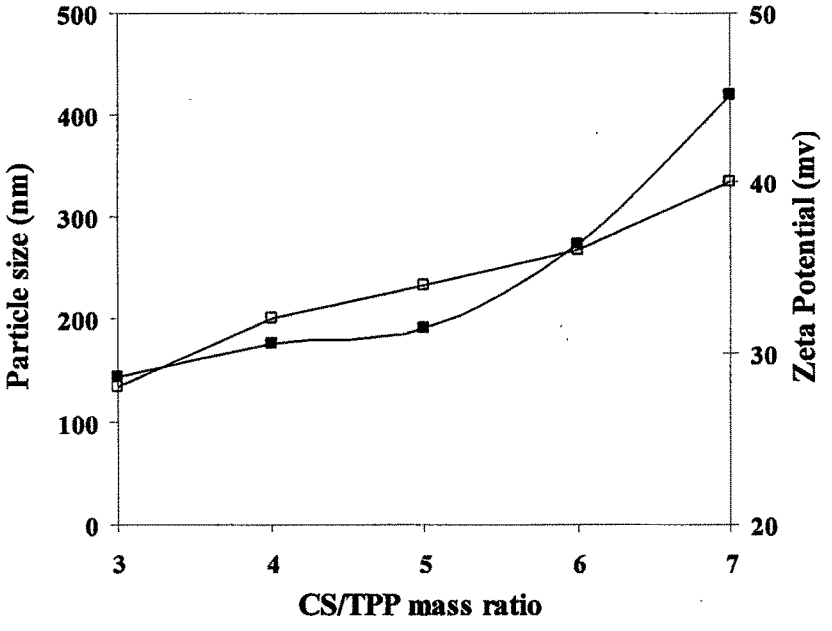

Figure 4.3 **Effect of CS/TPP mass ratio on (■) particle size and (□) zeta potential at CS concentration = 1.5 mg/ml, TPP concentration = 0.5 mg/ml.**

4.3.2 Optimization of conditions for the formation of venlafaxine hydrochloride loaded CS/TPP nanoparticles

After evaluating the effect of polymer concentration and mass ratio on particle size and zeta potential at fixed drug concentration, encapsulation efficiency of model bioactive molecule venlafaxine hydrochloride was further investigated. Venlafaxine hydrochloride loaded CS/TPP nanoparticles were obtained spontaneously upon addition of variable volumes of 0.5 mg/ml aqueous solution of TPP to the 4 ml of 1.5 mg/ml CS solution containing drug, under

magnetic stirring. To achieve the maximum encapsulation efficiency, different amounts of venlafaxine hydrochloride (200 µg/ml to 1000 µg/ml) were dissolved in chitosan solution (1.5 mg/ml) and then the venlafaxine hydrochloride loaded CS/TPP nanoparticles were prepared by addition of appropriate amount of TPP solution keeping the CS/TPP mass ratio 5:1. Effect of venlafaxine hydrochloride concentration on encapsulation efficiency, particle size and zeta potential of nanoparticles is illustrated in ***Figure 4.4 and 4.5.*** As seen from ***Figure 4.4*** with increase in drug concentration, encapsulation efficiency increases gradually up to 600 µg/ml and thereafter it decreases. Hence further study was carried out at 600 µg/ml concentration. With increasing concentration of venlafaxine hydrochloride from 200 to 1000 µg/ml, particle size was observed to increase almost linearly and marginal reduction was observed in zeta potential. ***(Figure 4.5).***

Chitosan concentration and CS/TPP mass ratio have specific effect on encapsulation efficiency of venlafaxine hydrochloride. It was observed that as chitosan concentration increases, venlafaxine hydrochloride encapsulation efficiency decreases from 74 % to 58 % ***(Figure 4.6).*** Similar observation was reported earlier for encapsulation of bovine serum albumin in CS/TPP nanoparticles. The reason behind such reduction in encapsulation efficiency is attributed to increase in viscosity of medium. The highly viscous nature of the gelation medium hinders the transfer of the drug molecules leading to reduction in encapsulation efficiency.

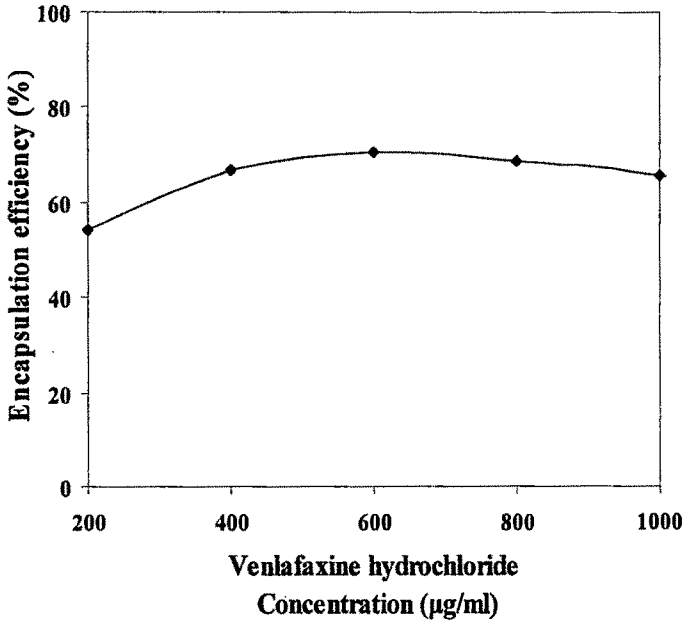

Figure 4.4 **Effect of venlafaxine hydrochloride concentration on encapsulation efficiency (CS/TPP mass ratio 5:1, pH= 5).**

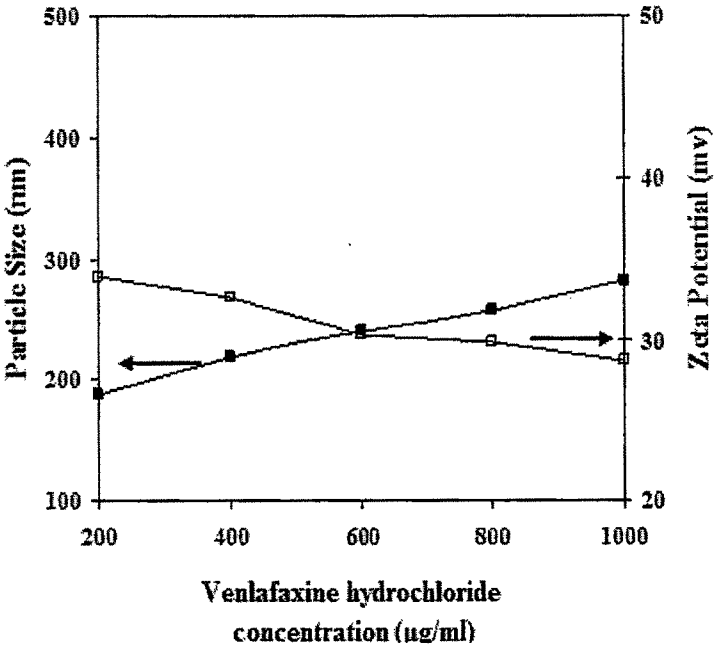

Figure 4.5 **Effect of venlafaxine hydrochloride concentration on (■) particle size and (□) zeta potential. (CS/TPP mass ratio 5:1, pH= 5).**

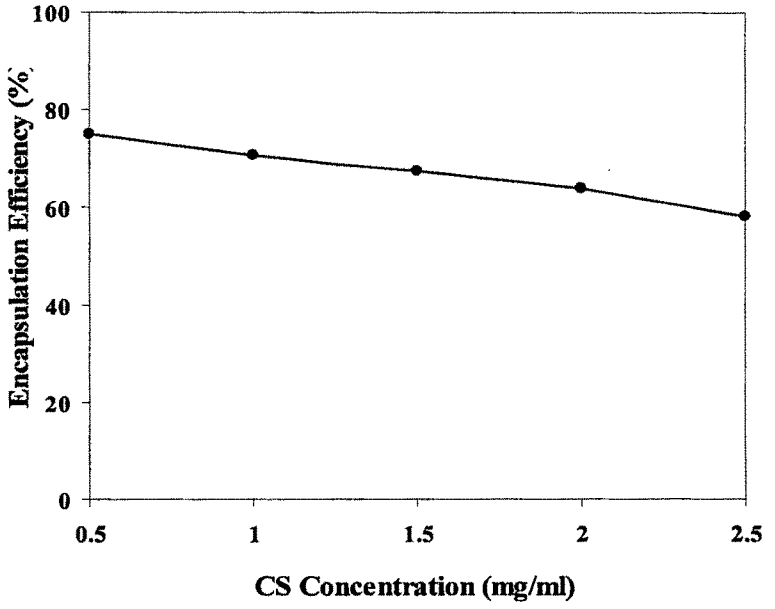

Figure 4.6 **Effect of chitosan concentration on encapsulation efficiency at CS/TPP mass ratio 5:1 and pH = 5.**

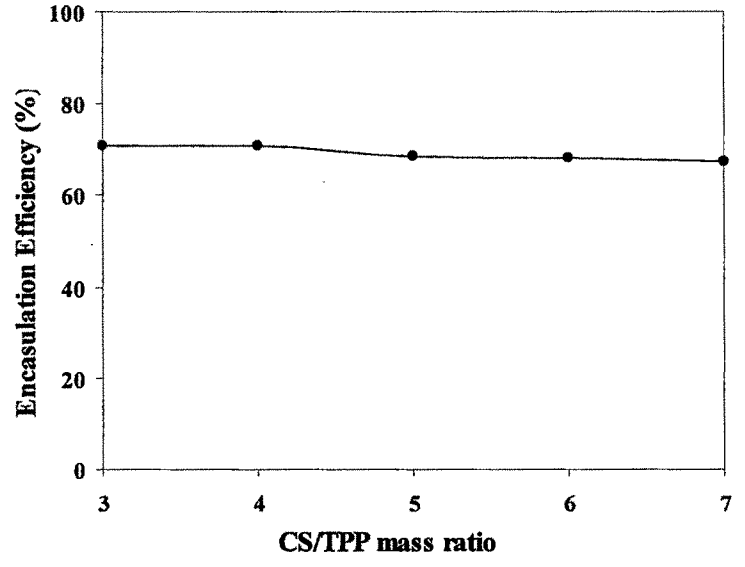

Figure 4.7 **Effect of CS/TPP mass ratio on encapsulation efficiency at chitosan and drug concentration 1.5 mg/mL and 0.6 mg/mL respectively at pH = 5.**

The effect of CS/TPP mass ratio on the encapsulation efficiency was studied at the mass ratios of 3:1, 4:1, 5:1, 6:1 and 7:1. Variation in CS/TPP mass

ratio did not show any effect on venlafaxine hydrochloride encapsulation ***(Figure 4.7).*** From the observations one can say that just by controlling the CS and drug concentration and CS/TPP mass ratio, one can control the encapsulation efficiency of venlafaxine hydrochloride in CS/TPP nanoparticles. Hence these results provide an important link in manipulation and optimization of the particle size, surface charge and also encapsulation efficiency for projected applications.

4.3.3 Optimization of conditions for the preparation of venlafaxine hydrochloride loaded PEG coated CS/TPP nanoparticles

PEG is widely used as coating material in pharmaceuticals, due to its proven safety potential attributed by its hydrophilicity, nontoxicity, absence of antigenicity and immunogenicity. Nanoparticles with the right coating can quickly slip through human mucus preventing the adherence of nanoparticles and viruses to the protein meshwork in the mucus, allowing them to become long circulating particles in physiological fluids. PEG coated CS nanoparticles containing venlafaxine hydrochloride were prepared at the conditions already optimized for CS/TPP nanoparticles as mentioned in section 4.2.2.C.

Effect of PEG concentration on particle size, zeta potential and encapsulation efficiency of venlafaxine hydrochloride in CS/TPP nanoparticles is illustrated in ***Figure 4.8 and 4.9.*** It was observed that particle size increases and zeta potential decreases with increase in PEG concentration ***(Figure 4.8).*** It has been previously reported that the incorporation of PEG in the gel system is through intermolecular hydrogen bonding between the electropositive quaternary amino groups of chitosan with electronegative hydroxyl groups of PEG.[70, 77]. The interaction between the oxygen atom from PEG and amino group from CS is weak but it still shows effect on the nanoparticle formation. Also, the addition of PEG reduces the positive charge on the nanoparticles. Quallec *et al*[78] also reported that the introduction of PEG can decrease significantly the positive surface charge on particles and noticeably improve their biocompatibility. While it was observed that, addition of PEG has negligible effect on encapsulation efficiency of venlafaxine hydrochloride ***(Figure 4.9).***

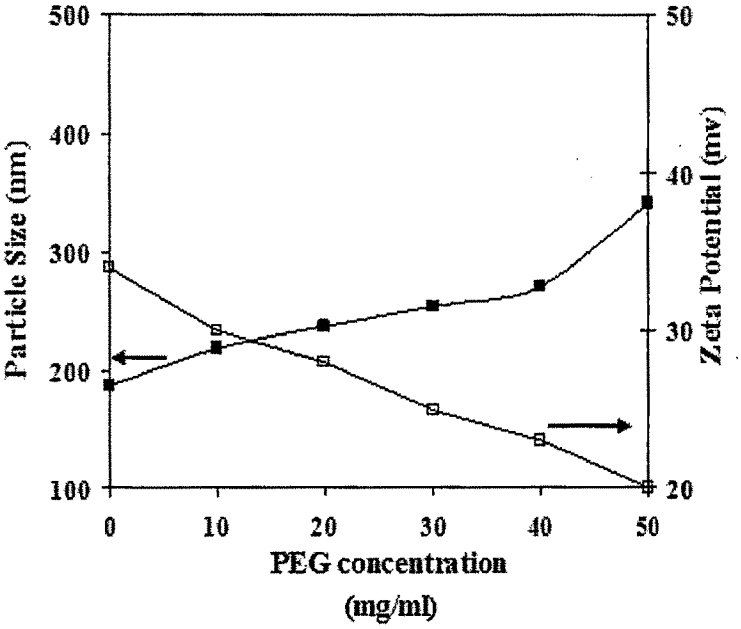

Figure 4.8 **Effect of PEG concentrations on (■) particle size and (□) zeta potential. (CS/TPP mass ratio = 5:1, venlafaxine hydrochloride concentration = 0.6 mg/mL at pH = 5).**

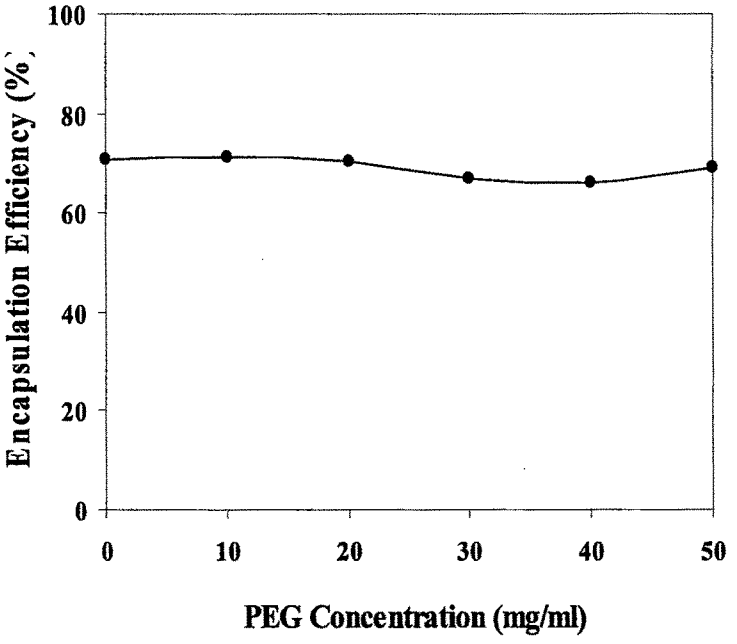

Figure 4.9 **Effect of PEG concentrations on encapsulation efficiency of venlafaxine hydrochloride in CS/TPP nanoparticles. (CS/TPP mass ratio = 5:1, venlafaxine hydrochloride concentration = 0.6 mg/mL at pH = 5).**

4.3.4 FTIR spectrometry

The nature of interactions between the drug and CS-TPP polymer was examined through FTIR spectrometry. In the mild acidic medium (pH = 5), where nanoparticle formation takes place, venlafaxine hydrochloride will be positively charged because of the presence of tertiary amino groups in their molecular structure. Hence during CS/TPP nanoparticle formation, besides hydrogen bonding, electrostatic interactions between TPP and drug molecules may take place. ***Figure 4.10*** shows FTIR spectra of chitosan, CS/TPP nanoparticles, venlafaxine hydrochloride, venlafaxine hydrochloride loaded CS/TPP nanoparticles and placebo PEG coated CS/TPP nanoparticles. Three characteristics absorption bands observed in ***Figure 4.10B*** at 3445, 1610 and 1325 cm^{-1} correspond to the -OH, $-NH_2$, and -C≡N groups of chitosan respectively. Shifting and broadening of band at 3445 cm^{-1} corresponding to hydroxyl group of CS, in CS/TPP nanoparticles to 3410 cm^{-1} ***(Figure 4.10 A)*** can be attributed to the possible intermolecular hydrogen bonding[79]. The observed shift in $-NH_2$ bending vibration from 1610 cm^{-1} to 1539 cm^{-1} and appearance of a new peak at 1630 cm^{-1} can be attributed to the linkage between phosphate groups of tripolyphosphate with ammonium groups of chitosan in nanoparticles. Similar observation was reported earlier by Calvo *et al*[35]. The presence of P=O group is indicated by the appearance of a peak at 1163 cm^{-1} ***(Figure 4.10A)***. These interactions reduce CS solubility and are responsible for CS separation from the solution in the form of micro/nanoparticles depending on the processing and formulation parameters. In the case of venlafaxine hydrochloride ***(Figure 4.10D),*** appearance of IR absorption band at 3352 cm^{-1} corresponds to the stretching vibrations of hydroxyl group. Bands at 2935, 1515-1450 and 1247 cm^{-1} are observed due to the stretching vibrations of $-CH_2$ group, benzene ring and methoxy group present in the drug structure. In the case of venlafaxine hydrochloride loaded CS/TPP nanoparticals ***(Figure 4.10C),*** existence of characteristic bands at 2935, 1514-1469 and 1247 cm^{-1} can be attributed to stretching vibrations of $-CH_2$, benzene ring and methoxy group of venlafaxine hydrochloride and bands at 3352, 1612 and 1170 cm^{-1} can be attributed to the presence of hydroxyl, primary amine and P=O groups from the CS/TPP nanoparticles, indicating the presence of drug in CS/TPP nanoparticles. As shown in the FTIR spectrum of placebo PEG coated CS/TPP nanoparticles

(Figure 4.10E), characteristic absorption bands at 2927, 1411 and 1108 cm^{-1} can be attributed to stretching and bending vibrations of $-CH_2$ group and presence of ether linkage in PEG, providing a confirmation of incorporation of PEG in the nanoparticle matrix.

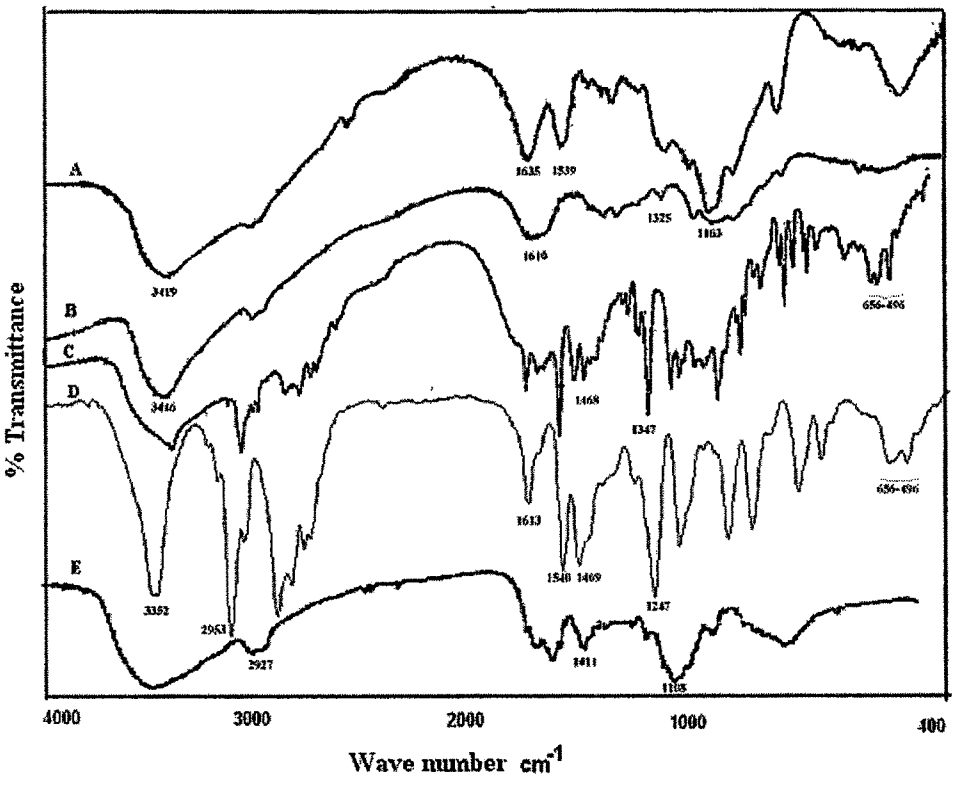

Figure 4.10 FTIR spectra of (A) CS/TPP nanoparticles, (B) chitosan, (C) venlafaxine hydrochloride loaded CS/TPP nanoparticles, (D) venlafaxine hydrochloride and (E) PEG coated CS/TPP nanoparticles.

4.3.5 DSC analysis

DSC studies were performed to understand the behavior of the cross-linked chitosan and physical state and interaction of the drug with the CS/TPP nanoparticles on application of thermal energy. Polysaccharides usually have a strong affinity for water and in solid state these macromolecules may have disordered structures that can be easily hydrated. The hydration properties of polysaccharides depend on primary and supramolecular structures. The endotherm

related to evaporation of water is expected to reflect the molecular changes brought in after cross-linking. To confirm the physical state and interaction of the drug with the CS/TPP nanoparticles, the plecebo nanoparticles, pure drug, physical mixture of drug and CS/TPP nanoparticles and venlafaxine hydrochloride loaded CS/TPP nanoparticles were examined by DSC. The DSC thermograms of CS/TPP nanoparticles (A), venlafaxine hydrochloride (B), venlafaxine hydrochloride loaded CS/TPP nanoparticles (C), physical mixture of CS/TPP nanoparticles and venlafaxine hydrochloride (D) and PEG coated CS/TPP nanoparticle (E) are given in ***Figure 4.11.*** The study revealed that unloaded nanoparticles showed a broad endothermic peak at 124 °C ***(Figure 4.11A)*** while in the case of pure venlafaxine hydrochloride ***(Figure 4.11B),*** a sharp peak observed at 217 °C corresponds to the melting point of venlafaxine hydrochloride. Similar observation was also reported by Ko *et* al[80]. In the case of venlafaxine hydrochloride loaded CS/TPP nanoparticles ***(Figure 4.11C),*** disappearance of the endothermic peak at 217°C corresponding to melting point of the venlafaxine hydrochloride indicates molecular level dispersion of drug in CS/TPP nanoparticle matrix, whereas, physical mixture of drug and nanoparticles ***(Figure 4.11D)*** shows separate characteristic endothermic peaks for drug and nanoparticles. Similar results are reported by Dhawal and Singla in the study of nifedipine loaded chitosan microspheres[81]. They have reported that at 1.84 % drug loading, drug remains molecularly dispersed in microspheres. In the case of PEG coated CS/TPP nanoparticles, observed broad endothermic peak for CS/TPP nanoparticles at 124 °C was shifted to 116 °C ***(Figure 4.11E).*** The decrease in the position of endothermic peak for PEG coated CS/TPP nanoparticles supports interaction between chitosan and PEG[33] indicating very good compatibility of PEG with CS matrix.

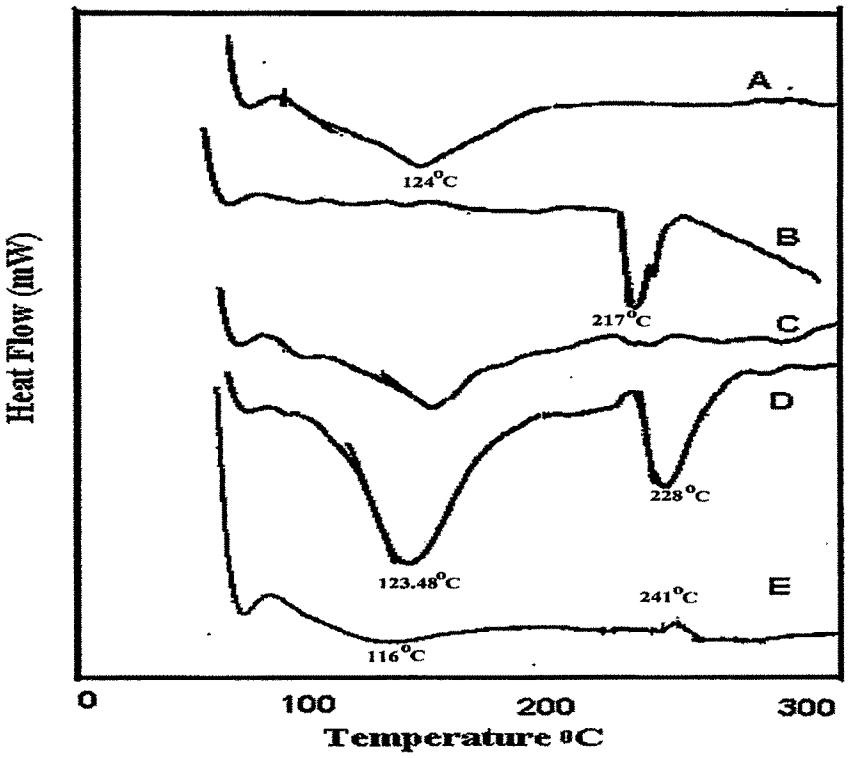

Figure 4.11 DSC thermograms of (A) CS/TPP nanoparticles, (B) venlafaxine hydrochloride, (C) venlafaxine hydrochloride loaded CS/TPP nanoparticles, (D) physical mixture of venlafaxine hydrochloride and CS/TPP nanoparticles and (E) placebo PEG coated CS/TPP nanoparticles.

4.3.6 XRD analysis

The X-ray diffraction patterns of venlafaxine hydrochloride, chitosan, CS/TPP nanoparticles and venlafaxine hydrochloride loaded CS/TPP nanoparticles are shown in ***Figure 4.12***. XRD spectrum of chitosan ***(Figure 4.12B)*** showed two prominent crystalline peaks at 10.375° (2θ) and 20.175° (2θ). In the case of CS/TPP nanoparticles ***(Figure 4.12C),*** there was significant decrease in the intensity of characteristic peaks of chitosan, which is in agreement with the results reported by Wan *et al*[82]. The distinct differences in the diffraction patterns of CS and CS/TPP nanoparticles could be attributed to the modification in

the arrangement of molecules in the crystal lattice. From the XRD patterns of venlafaxine hydrochloride ***(Figure 4.12A)*** and venlafaxine hydrochloride loaded CS/TPP nanoparticles ***(Figure 4.12D)***, molecular level dispersion of venlafaxine hydrochloride in CS/TPP nanoparticles is clearly indicated from the disappearance of XRD bands of the drug appearing at 2θ = 8.3, 12.66, 13.49, 15.56, 20.32, 25.00, 28.48 and 35.56°. Sarmento *et al*[83] in the study of dorzolamide and pramipexole in CS/TPP nanoparticles have also reported similar observation. From XRD data, they have reported that, Pramipexole probably formed a molecular level dispersion or an amorphous nano-dispersion within the CS matrix of the nanoparticles. On the other hand they have observed Pramipexole, Dorzolamide crystallizes out during its entrapment in the CS nanoparticles.

The X-ray diffraction patterns of chitosan, PEG and PEG coated CS/TPP nanoparticles are shown in ***Figure 4.13.*** The XRD pattern of chitosan consisted of two typical crystalline peaks at 10.775° and 19.775° while PEG had typical crystalline peaks at 13.175, 19.075°, 23.975°, 26.6° and 37.975° because of its close molecular packing and regular crystallization. In the case of X-ray diffraction patterns of PEG coated CS/TPP nanoparticles, it was observed that the diffraction peaks of chitosan at 10.775° and 19.775° get reduced and new diffraction peaks appeared at 20.175° and 23.975°. This can be explained through the strong interaction between chitosan and PEG which has weakened the close packing of the chitosan molecules and has created new crystallites. In other words, the results of X-ray diffraction reinforce the existence of good compatibility between the CS with PEG[84].

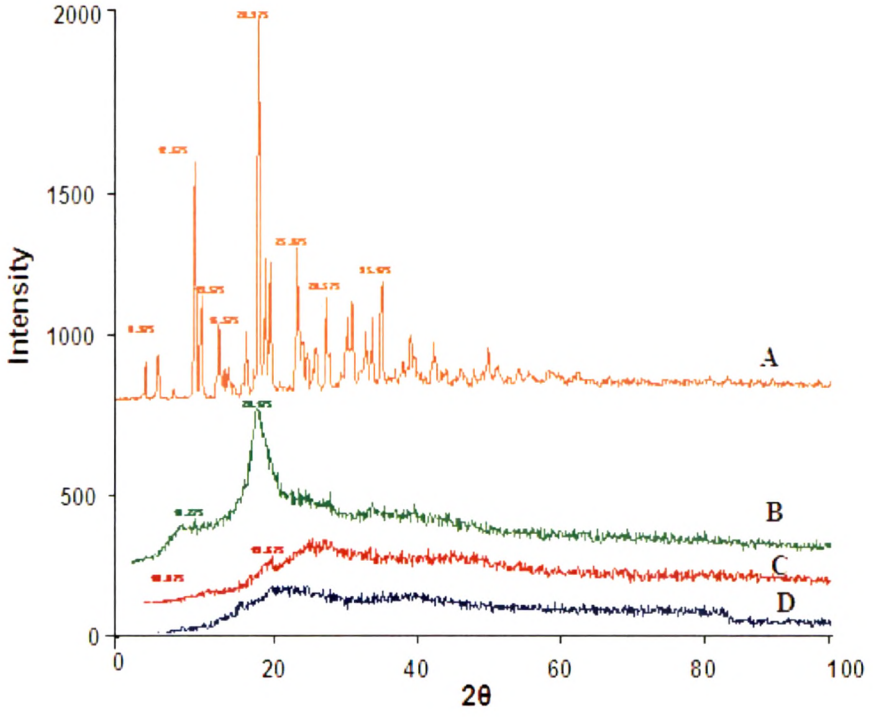

Figure 4.12 **XRD patterns of (A) venlafaxine hydrochloride, (B) chitosan, (C) CS/TPP nanoparticles and (D) venlafaxine hydrochloride loaded CS/TPP nanoparticles**

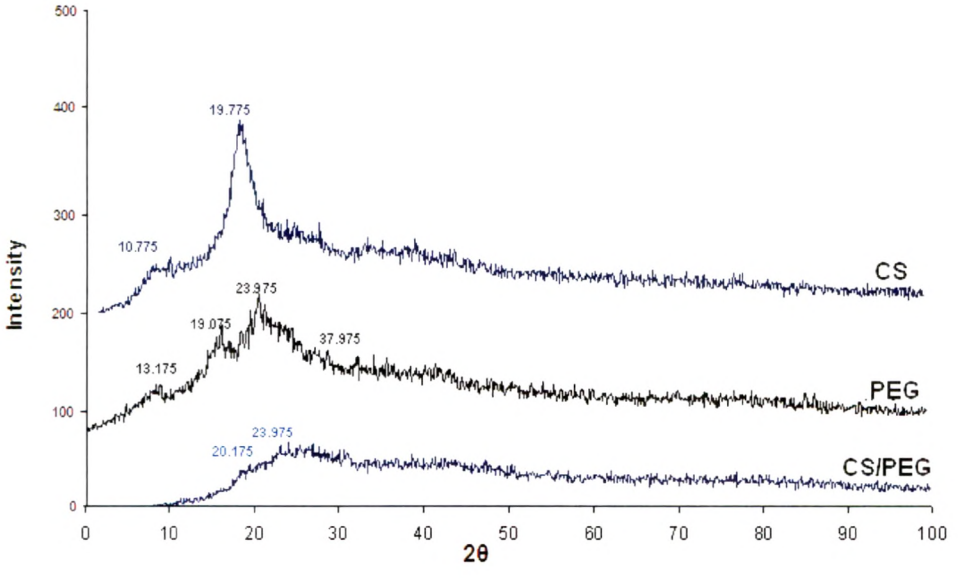

Figure 4.13 **XRD patterns of chitosan, PEG and PEG coated CS/TPP nanoparticles**

4.3.7 Transmittance electron micrography (TEM)

Transmittance electron micrographic (TEM) images of plecebo nanoparticles and venlafaxine hydrochloride loaded CS/TPP nanoparticles prepared at the CS/TPP mass ratios of 5:1 under magnetic stirring for a period of 30 minutes at room temperature (30 ± 2 °C) are given in ***Figure 4.14.*** It was observed that, placebo nanoparticles exhibit nearly spherical morphology with particle size of ~250 nm ***(Figure 4.14A)*** for the prescribed experimental conditions. While venlafaxine hydrochloride loaded CS nanoparticls ***(Figure 4.14B)*** exhibit some irregularity in shape and size. The particle size was observed in the range of 300 nm. Increase in size may be due to loading of drug in the CS/TPP nanoparticles. The observed size of these nanoparticles from TEM analysis is in good agreements with the results obtained from dynamic light scattering studies. TEM image of PEG coated CS/TPP nanoparticles is illustrated in ***Figure 4.14 C & D.*** Spherical particles with smooth and uniform coating on the surface were observed and the overall size of the particles was observed to be larger as compared to unmodified nanoparticles.

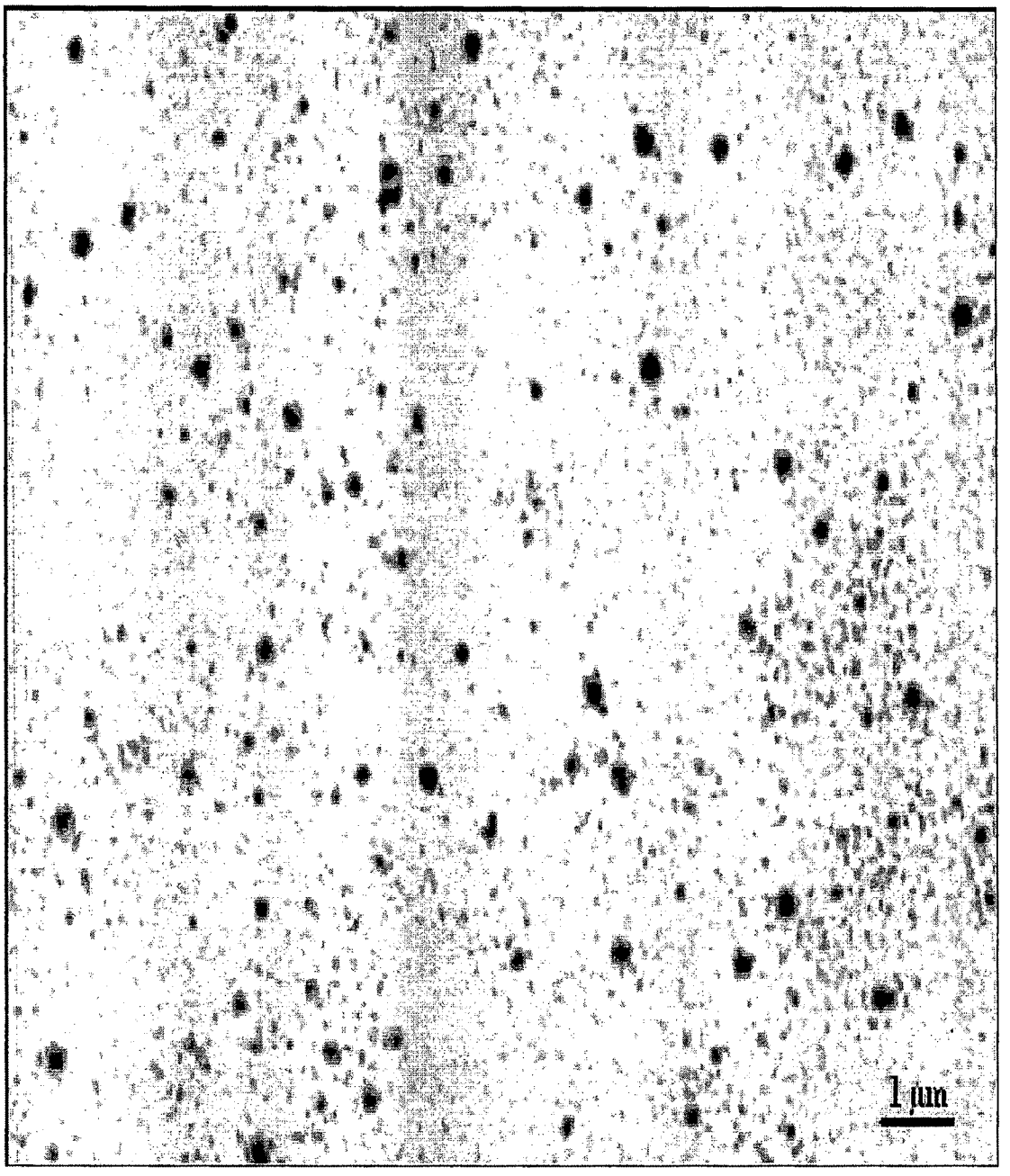

(A) TEM images of CS/TPP nanoparticles

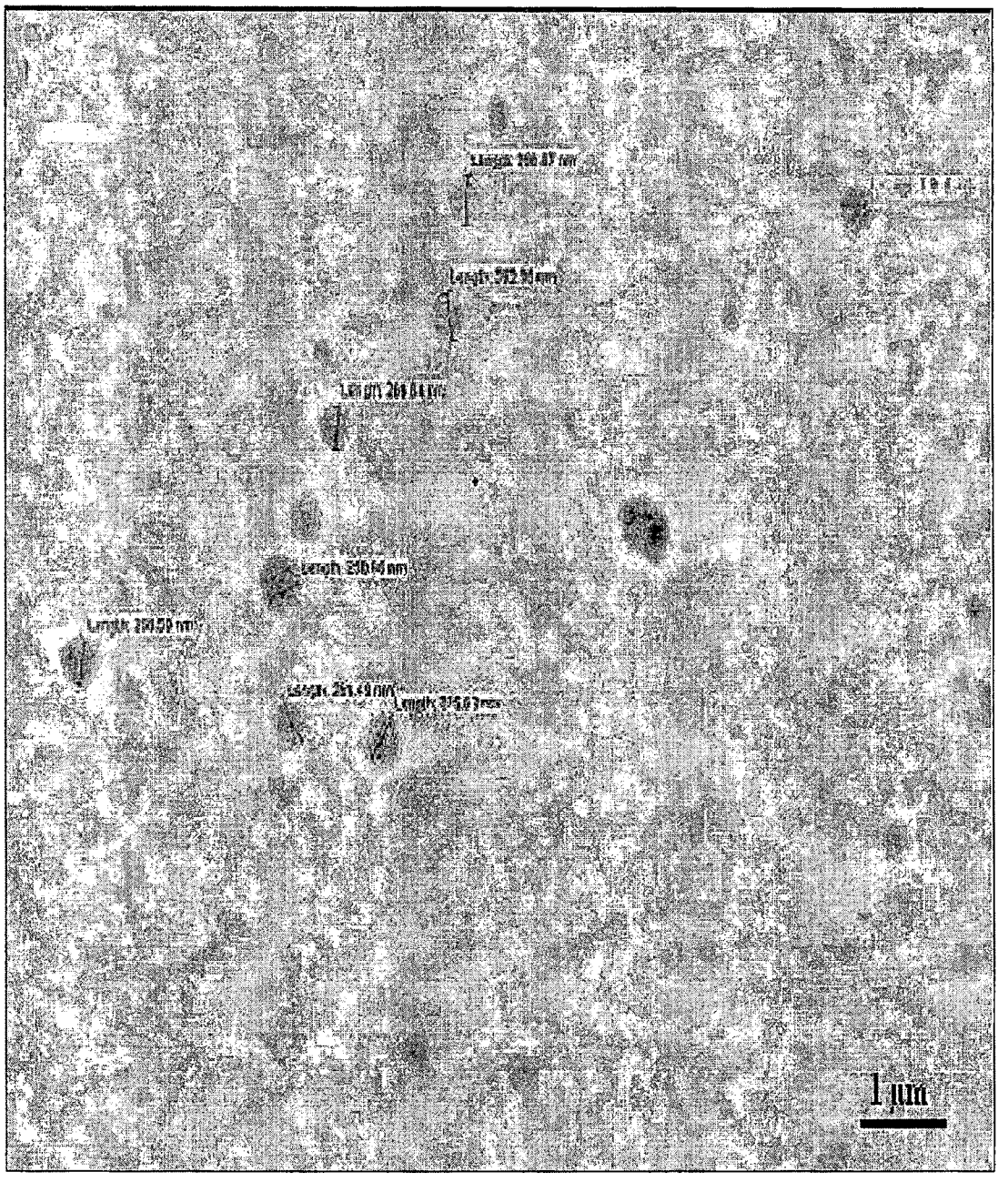

(B) TEM images of venlafaxine hydrochloride loaded CS/TPP nanoparticles

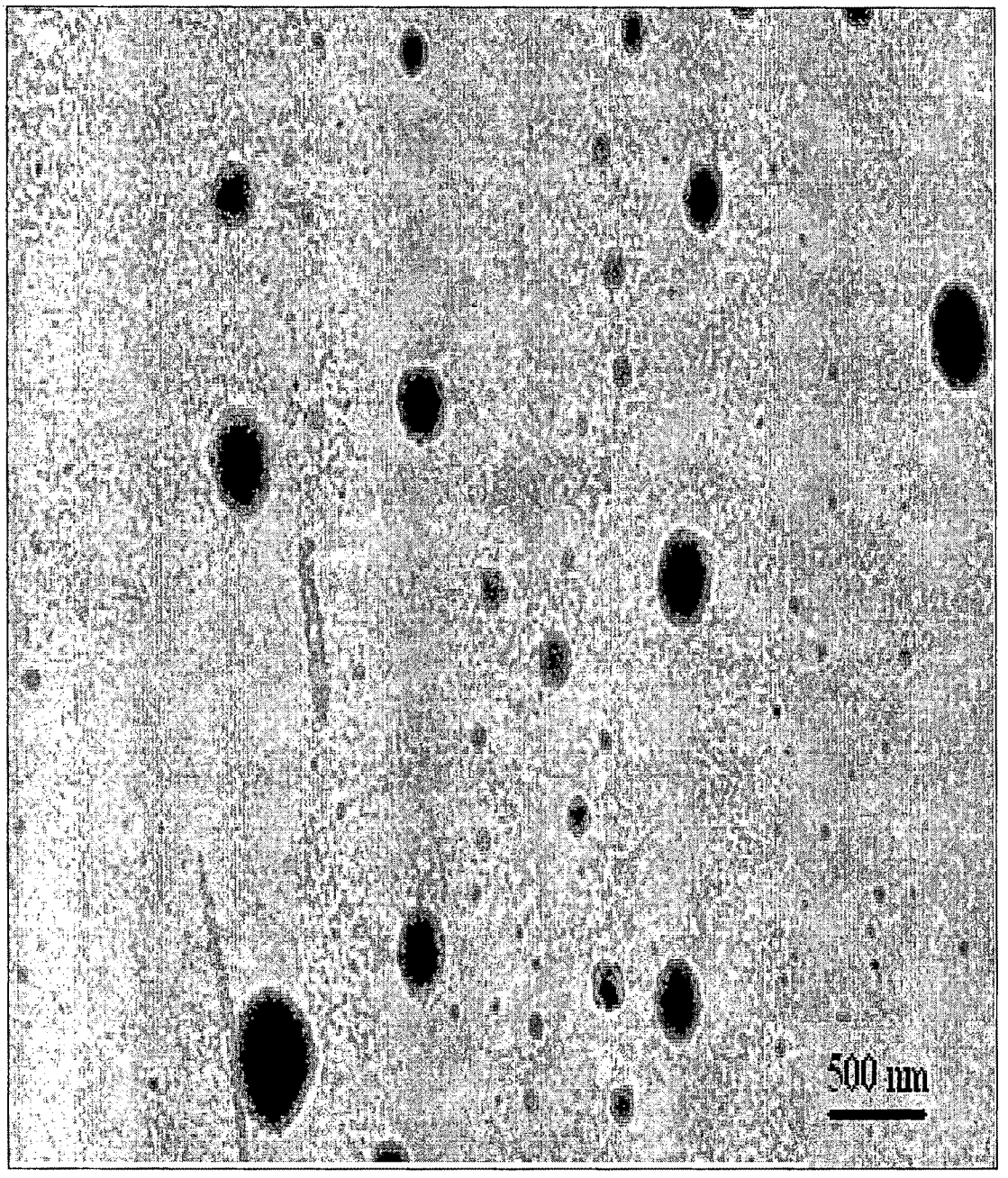

(C) TEM images of PEG coated CS/TPP nanoparticles

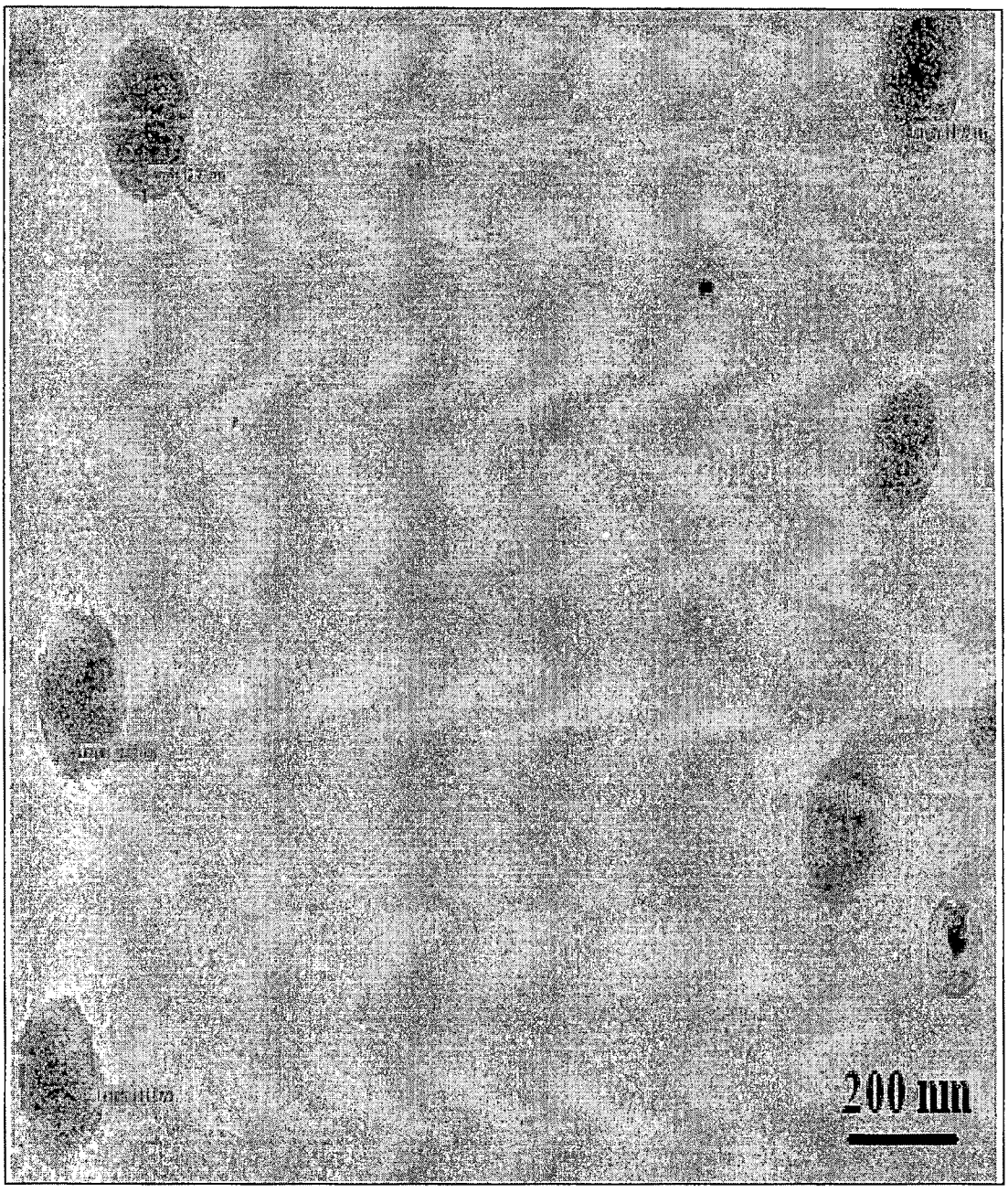

(D) TEM images of PEG coated CS/TPP nanoparticles

Figure 4.14 TEM images of (A) CS/TPP nanoparticles, (B) venlafaxine hydrochloride loaded CS/TPP nanoparticles, (C, D) PEG coated CS/TPP nanoparticles synthesized at CS/TPP mass ratio = 5:1, venlafaxine hydrochloride = 0.6 mg/ml, PEG = 30 mg/ml at pH = 5.

4.3.8 XPS analysis

To prove the presence of PEG coating on the surface of CS/TPP nanoparticles, XPS analysis was carried out. XPS survey scan of PEG and chitosan (CS), indicated presence of C (1S) and O (1S) photoelectron line for PEG and C (1S), N (1S) and O (1S) photoelectron line for CS. As nitrogen photoelectron lines appear only in CS spectrum, presence of nitrogen and its quantitative comparison with carbon atoms was used as a probe for PEG coating on CS/TPP nanoparticles. Yu *et al*[85] reported that photoelectron line of C (1S) was observed at 285.0 ± 0.1 eV. ***Figure 4.15(B)*** shows XPS scan of CS/TPP nanoparticles and PEG coated CS/TPP nanoparticles, wherein a decrease in the intensity of N (1S) has been noticed along with the increase in C (1S) and O (1S) photoelectron line intensities. ***Figure 4.15(A)*** shows quantitative XPS comparison of carbon and nitrogen on the surface of CS/TPP nanoparticles and PEG coated CS/TPP nanoparticles. This data clearly indicates increase in carbon on the surface of coated samples. However, considerable decrease in nitrogen was seen on the surface of coated sample compared to CS/TPP nanoparticles surface. These results clearly indicate that nitrogen is buried below PEG and hence XPS signals in coated samples indicate more of PEG nano layer coated above CS/TPP nanoparticles. Surface composition, O/N and C/N atomic ratio of PEG coated CS/TPP nanoparticles and CS/TPP nanoparticles are given in ***Table 4.2***. High resolution C (1S) spectra of PEG, PEG coated CS/TPP nanoparticles and CS shown as a insets of ***Figure 4.15A,*** show presence of C-C and C-H functionality at 285.0 ± 0.1 eV[85] and C-O-C, C-OH, and C-N functionalities[86, 87] at 286.6 ± 0.1 eV. It is worth mentioning that C (1S) spectra shape shown in quantitative data is broad because these functionalities are not resolved properly in low resolution data. Thus XPS data shown in ***Figure 4.15 A & B*** indicate that although nitrogen signal is very small, it is visible in PEG coated CS/TPP nanoparticles layer. This suggests that CS/TPP nanoparticles are coated with monolayer of PEG as it is also seen in TEM picture ***(Figure 4.14 C & D).***

Results obtained from FTIR, DSC and particle size analysis also support the interaction and incorporation of PEG in CS matrix, as discussed earlier and summarized here;

- Presence of characteristic absorption bands at 2927 cm^{-1}, 1411 cm^{-1} and 1108 cm^{-1} correspond to stretching and bending vibrations of $-CH_2$ group and presence of ether linkage due to PEG. (***Figure 4.10E***)
- Shifting of endothermic peaks from 124 °C to 116 °C. (***Figure 4.11E***)
- Increase in particle size with addition of PEG in CS/TPP nanoparticles respectively providing a confirmation of incorporation of PEG in the nanoparticle matrix. (***Figure 4.8***)

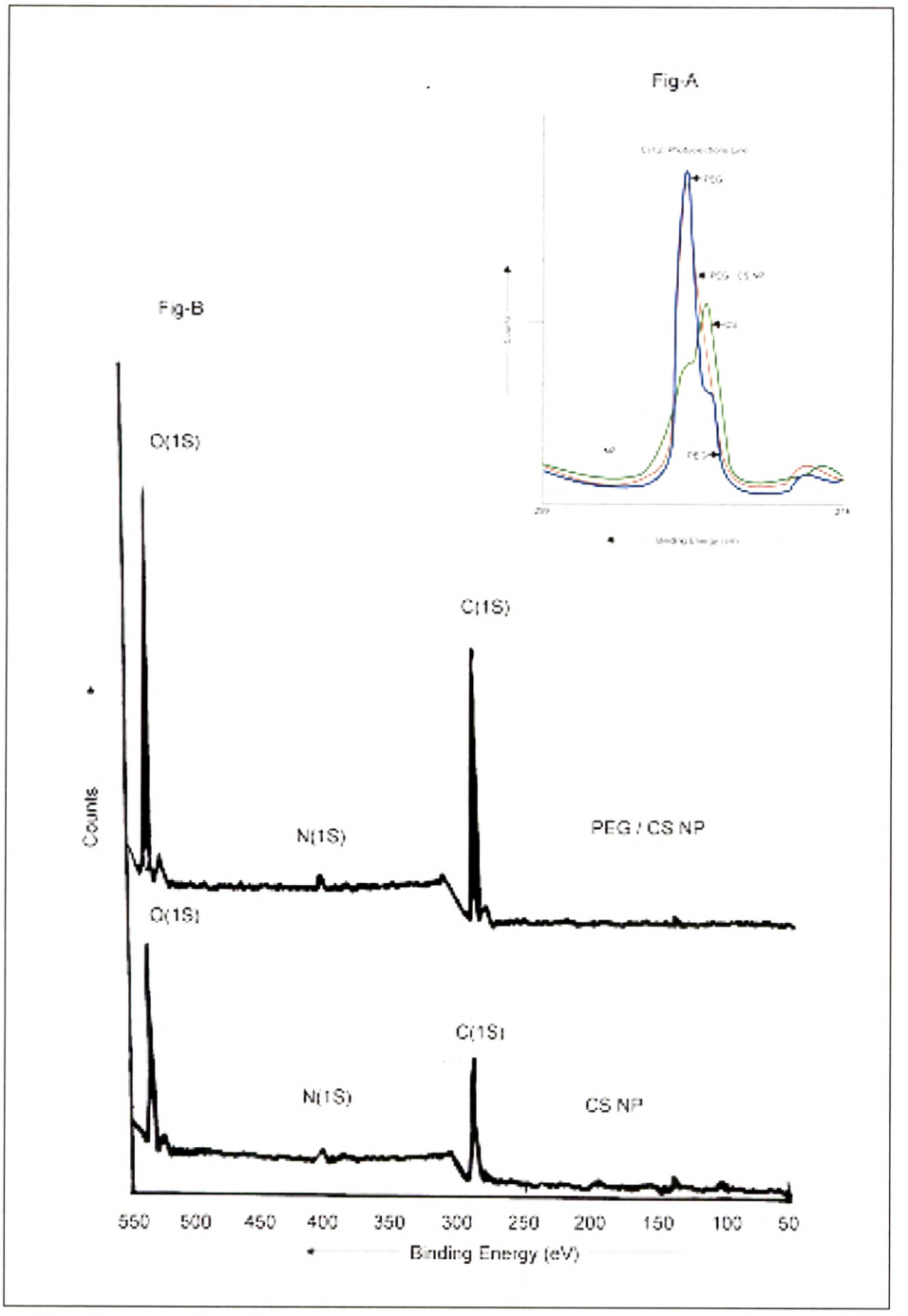

Figure 4.15 **XPS analysis of CS, PEG, CS/TPP and PEG coated CS/TPP nanoparticles. (A) High resolution C (1S) photoelectron line showing carbon functionalities and relative composition in CS, PEG and PEG coated CS nanoparticles, (B) XPS survey scan of CS/TPP nanoparticles & PEG coated CS/TPP nanoparticles.**

Table 4.2 XPS composition of CS/TPP nanoparticles & PEG coated CS/TPP nanoparticles.

Sample	C (Atomic %)	N (Atomic %)	O (Atomic %)	C / N (Atomic ratio)	O / N (Atomic ratio)
CS/TPP nanoparticles	63.2	6.2	30.6	10.2	4.9
PEG coated CS/TPP nanoparticles	67.1	1.7	31.2	39.5	18.4

4.3.9 In vitro release study

Venlafaxine hydrochloride is highly soluble in water and due to very short steady state elimination half-life (3-4 h)[88, 89] it is very difficult to develop a pharmaceutical formulation with a slow dissolution rate of freely soluble drug. Hence in order to keep a stable therapeutic level, multiple daily administrations of venlaflaxine hydrochloride based formulations are needed. Both the immediate and extended release formulation have efficacy in reducing symptoms of depression. However, the extended release formulation has advantages in increasing patient compliance. Besides from the marketed formulations, many researchers have tried to prepare controlled release formulation of venlafaxine hydrochloride. Yang and Lopina[90] developed extended release formulation of venlafaxine hydrochloride based on polyamidoamine dendrimers and reported that, the drug was released in a sustained way and almost half of the conjugated drug was released within 18 h. They also correlate the effect of percentage loading on burst release, i.e. at 75 mg venlafaxine loaded matrix, 92 % of drug was released within 6 h, while for 8 mg venlafaxine hydrochloride loaded matrix, only 50% of drug was released. Hence here we have tried to use selected CS/TPP nanoparticles and PEG coated CS/TPP nanoparticles for the encapsulation of venlafaxine hydrochloride and study of in-vitro release of venlafaxine hydrochloride from them. ***Figure 4.16A*** shows the release profile of venlafaxine hydrochloride from CS/TPP and PEG coated CS/TPP nanoparticles. It was

observed from the plots that, in- vitro release of venlafaxine hydrochloride shows a very rapid initial burst followed by a slow drug release at 7.4 pH. Generally the drug release is due to the diffusion of drug molecules through the matrix or due to degradation of polymeric matrix. In the present case initial burst release of drug molecules from nanoparticles can be attributed to the presence of drug molecules near the periphery of the nanoparticles, which diffuse in the surrounding medium due to rapid penetration of release medium in the hydrophilic nanoparticles. The release rate was observed to be slow for PEG coated CS/TPP nanoparticles as compared to unmodified nanoparticles due to the presence of surface cross linking of PEG, which produces hindrance for the diffusion of drug molecule in release medium[91]. ***Figure 4.16B*** shows the effect of drug concentration on extent of release of the drug. It was observed that, as we increase the initial drug concentration in the nanoparticles, its release rate is also observed to increase. ***Figure 4.16C*** shows release profile with respect to chitosan concentration at constant CS/TPP mass ratio (5:1) and drug concentration (0.6 mg/ ml). It was observed that, total cumulative release reduces from 90 % to 56 % when the chitosan concentration increases from 0.5 mg/mL to 2.5 mg/mL. This can be attributed to the increased viscosity of CS solution allowing the formation of denser CS/TPP particles, resulting grater crosslink density with less swelling ability and thereafter reducing venlafaxine hydrochloride release[92]. It was also reported by Hu *et al*[79] that higher CS concentration leads to larger particles and hence drug molecules are likely to bind to multiple sites of CS/TPP nanoparticles, resulting into slow release. In addition, membrane permeability of the CS/TPP nanoparticles would be theoretically lower with increasing CS concentration due to increased chain packing and rigidity, as well as interchain bonding. All of the above factors result in reduced burst effect and slower release kinetics of the drug molecules. Similar results are reported earlier[79, 92]. ***Figure 4.16 D*** shows the effect of CS to TPP mass ratio on the release profile. It was observed that when CS to TPP mass ratio decreases from 7 to 3, total cumulative release increases from 78 to 97 %. Hence at low chitosan to TPP mass ratio, faster release rate is observed as compared to higher CS to TPP mass ratio.

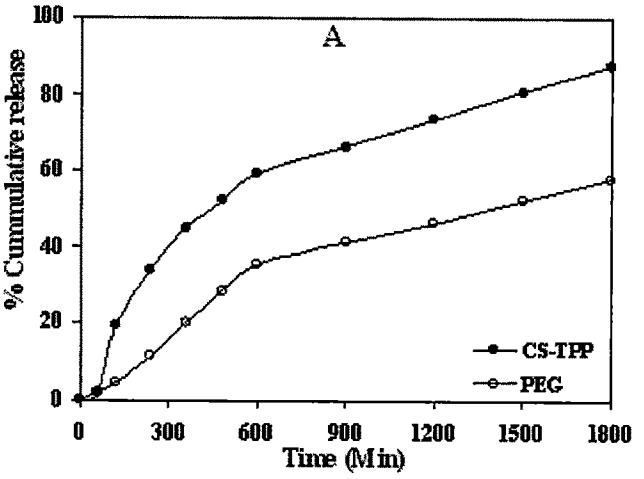

Figure 4.16 A **In-vitro release of venlafaxine hydrochloride from CS/TPP and PEG coated CS/TPP nanoparticles synthesized at CS/TPP mass ratio 5:1. CS, PEG and drug concentrations 1.5 mg/ml, 30 mg/ml, 600 µg/ml respectively.**

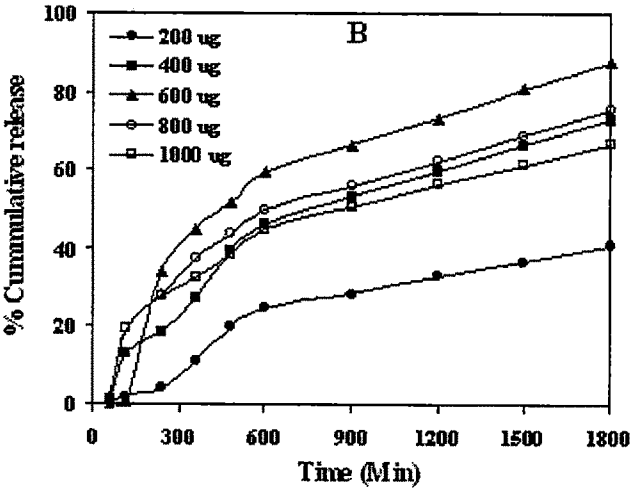

Figure 4.16 B **Effect of venlafaxine hydrochloride concentration on the percentage cumulative release from CS/TPP nanoparticles synthesized at CS/ TPP mass ratio: 5:1, pH = 5).**

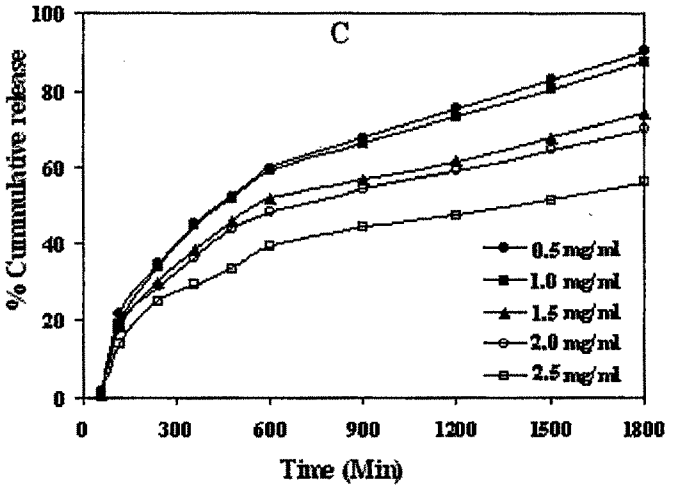

Figure 4.16 C **Effect of chitosan concentration on the percentage cumulative release from CS/TPP nanoparticles synthesized at CS/ TPP mass ratio: 5:1, pH = 5.**

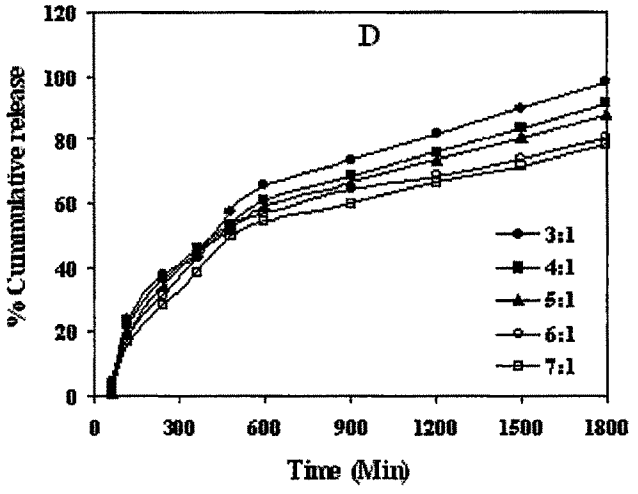

Figure 4.16 D **Effect of CS/TPP mass ratio on the percentage cumulative release from CS/TPP nanoparticles. Concentration of CS and drug = 1.5 mg/mL and 0.6 mg/ml respectively.**

Figure 4.16 **In-vitro release profile of venlafaxine hydrochloride from CS/TPP nanoparticles.**

4.4 Conclusion

From the present studies of encapsulation of model drug venlafaxine hydrochloride, we can conclude that the CS/TPP nanoparticles and PEG coated CS/TPP nanoparticles can offer some attractive features which favor them as a promising carriers for the further study of charged therapeutic agents. The main features include,

- Formation of nanoparticles can be achieved under extremely mild conditions, without affecting structure and properties of drug encapsulated.
- Easy modulation of particle size and surface charge through control of experimental conditions such as chitosan, PEG concentration and CS/TPP mass ratio, which can have critical role in their applications.
- Molecular level dispersion of venlafaxine hydrochloride within the nanoparticles was confirmed from XRD and DSC analysis.
- Encapsulation efficiency upto 70 ± 5 % was observed for CS/TPP nanoparticles at 0.6 mg/ml drug concentration.
- Better encapsulation efficiency of drug and superior physicochemical properties of nanoparticles were observed at lower chitosan concentration and lower chitosan to TPP mass ratio at specific drug concentration.
- Addition of PEG during nanoparticle formation has no effect on encapsulation efficiency of drug but shows delayed release of entrapped drug molecules due to increased bulk density and coating as observed in TEM on the nanoparticles.
- PEG coating on the surface of CS/TPP nanoparticles confirmed through XPS and TEM investigation.

All these observations make the system as interesting carrier for drug delivery applications.

4.5 References

1. Illum L., *Pharm. Res.*, 1998, **15,** 1326.
2. Synowiecki J., Ali Al-Khateeb N., *Cri. Rev. Food Sci. & Nutr.*, 2003, **43,** 145.
3. Tharanathan R.N., Kittur F. S., *Cri. Rev. Food Sci. & Nutr.*, 2003, **43,** 61.
4. Ravi Kumar M.N.V, Muzzarelli R.A.A., *Chem. Rev.*, 2004, **104,** 6017.
5. Ratajska M., Strobin G., Wiśniewska-Wrona M., Ciechańska D., Struszczyk H., Boryniec S., Biniaś D., Biniaś W., *Fibers & Textiles in Eastern Europe.*, 2003, **11,** 42.
6. Crini G., *Prog. Polym. Sci.*, 2005, **30,** 38.
7. Babel S., Kurniawan T.A., *J. Hazardous Mater.*, 2003, **97**, 219.
8. Dutta P., Ravikumar M.N.V., Dutta J., *J Macromol. Sci. Part C – Polym. Rev.*, 2002, **42**, 307.
9. Singla, A.K., Chawla M., *J. Pharm. Pharmacol.*, 2001, **53,** 1047.
10. Shepherd R., Reader S., Falshaw A., *Glycoconj. J.*, 1997, **14,** 535.
11. Illume L., *J. Pharma. Sci.*, 2007, **96**, 473.
12. Ngah W.S.W., Ghani S.Ab., Kamari A., *Bioresourse Tech.*, 2005, **96**, 443.
13. Gumusderelioglu M., Agi P., *React. Func. Polym.*, 2004, **61**, 211.
14. Nakajima M., Atsumi K., Kifune K., *Chitin, chitosan and related enzymes.*, (Eds.), Zikakis J.P. Acedemic Press, Harcourt Brace Janovich: New York, 1984, 407-410.
15. Douglas B., De Odilio., De B.G., *Biomacromolecules.*, 2007, **41**, 198.
16. Rinaudo M., *Prog. Polym. Sci.*, 2006, **31,** 603.
17. Wang Y.L., Gu H.Y., Su Z.G., Ma H.G., *Int. J. Pharm. Sci.*, 2006, **311,** 187.
18. Tozaki H., Komoike J., Tada C., Maruyama. T., Terabe A. Suzuki T., Yamamoto A., Muranishi S., *J. Pharma. Sci.*, 1997, **86,** 1016.
19. Liu Z.D., Sheu T.M., Chen H.C., Yang R.Y., Ho O.H., *J. Control. Release.*, 2007, **118**, 333.
20. Kristl J., Smid-Korbar J., Strue E., Schara M., Rupprecht H., *Int. J. Pharm. Sci.*, 1993, **99**, 13.
21. Portero A., Teijeiro-Osorio D., Alonso M.J., Remuñán-López C., *Carbohydrate Polym.*, 2007, **68**, 617.

22. Tobio M., Gref A., Sanchez S., Langer R., Alonso M., *Pharm. Res.*, 1998, **15,** 270.
23. Li S., He Y., Li C., Liu X., *Colloid. & Polym. Sci.*, 2005, **283,** 480.
24. Venier-Julienne M.C., Benoit J. P., *Pharma. Acta. Helv.*, 1996, **71,** 121.
25. De T.K., Hoffman A.S., *Art. Cells, Blood Subs and Immob Biotech.*, 2001, **29,** 31.
26. Peppas L.B., *Int. J. Pharm. Sci.*, 1995, **116,** 1.
27. Calvo P., Vila-Jato J.L., Alonso M. J., *J. Pharm. Sci.*, 1996, **85,** 530.
28. Couvreur P., Dubernet C., Puisieux F., *Eur. J. Pharm.*, 1995, **41,** 2.
29. Couvreur P., Kante B., Roland M., Goit P., Bauduin P., Speiser P., *J. Pharm. Pharmacol.*, 1979, **31,** 331.
30. Gref R., Minamitake Y., Peracchia M.T., Trubetskoy V., Torchilin V.P., Langer R., *Science.*, 1994, **18,** 1600.
31. Schroeder U., Sommerfeld P., Sabel B.A., *Peptide.*, 1998, **19,** 777.
32. Julienne M.C., Alonso M.J., Amoza J.L G., Benoit J. P., *Drug Dev. Ind. Pharm.*, 1992, **10,** 1063.
33. Ibrahim H., Bindschaedler C., Doelker E., Buri P., Gurny R., *Int. J. Pharm. Sci.*, 1992, **87,** 239.
34. Leroux J.C., Allemann E., Doelker E., Gurny R., *Eur. J. Pharm. Biopharm.*, 1995, **41,** 14.
35. Calvo P., Remunan-Lopez C., Vila-Jato J.L., Alonso M.J., *J. Appl. Polym. Sci.*, 1997, **63,**125.
36. Genta I., Castantini M., Asti A., Conti B., Montanari L., *Carbohydrate Polym.*, 1998, **36,** 81.
37. Bodmeier R., Chen H., Paeratakulm O., *Pharm. Res.*, 1989, **6,** 413.
38. Sashiwa H., Aiba S.I., *Prog. Polym. Sci.*, 2004, **29,** 887.
39. Baxter A., Dillon M., Taylor K.D.A., Roberts G.A.F., *Int. J. Biol. Macromol.*, 1992, **14,** 166.
40. Zhang Y., Yang Y., Tang K., Hu X., Zou G., *J. Appl. Polym. Sci.*, 2008. **107,** 891.
41. Papadimitriou S., Bikiaris D., Avgoustakis K., Karavas E., Georgarakis M., *Carbohydrate Polym.*, 2008, **73,** 44.
42. Tsai M.N., Bai S.W., Chen R.H., *Carbohydrate Polym.*, 2007, **342,** 87.
43. Liu H., Chen B., Mao Z., Gao C., *J. Appl. Polym. Sci.*, 2007, **106,** 4248.

44. Sun Y., Wan A., *J. Appl. Polym. Sci.*, 2007, **105**, 552.

45. Gan Q., Wang T., *Colloid. & Surf. B: Biointerfaces.*, 2007, **59**, 24.

46. Lin Y.H., Mi F.L., Chen C.T., Chang W.C., Peng S.F., Liang H. F., Sung H.W., *Biomacromolecule.*, 2007, **8,** 146.

47. Sarmento B., Ferreira D., Veiga F., Ribeiro A., *Carbohydrate Polym.*, 2006, **66**, 1.

48. Bhumkar D.R., Pokharkar V.B., *AAPS Pharm. Sci. Tech.*, 2006, **7**, 50.

49. Bodnar M., Hartmann J.F., Borbely J. *Biomacromolecules.*, 2005, **6**, 2521.

50. Wu Y., Yang W., Wang C., Hu J., Fu S., *Int. J. Pharm.*, 2005, **295,** 235.

51. Boonsongrit Y., Mitrevej A., Muller, B.W., *Eur. J. Pharm. Biopharma. Sci.*, 2005, **62,** 267.

52. Grenha A., Seijo B., Remunan-Lopez C., *Eur. J. Pharm. Sci.*, 2005, **25,** 427.

53. Aktas Y., Andrieux K., Alonso M.J., Calvo P., Neslihan G. R., Couvreur P., Capan Y., *Int. J. Pharma.*, 2005, **298,** 378.

54. Lopez-Leon T., Carvalho E.L.S., Seijo B., Ortega-Vinuesa J.L., Bartos-Gonzalez D., *J. Colloid. & Interface Sci.*, 2005, **283,** 344.

55. Xu Y., Du Y., *Int. J. Pharma.*, 2003, **250**, 215.

56. Dyer A.M., Hinchcliffe M., Watts, P., Castile J., Jabbal-Gill I., Nankervis R., Smith A., Illum L., *Pharm. Res.*, 2002, **19,** 998.

57. Janes K.A., Fresneau M.P., Marazuela A., Fabra A., Alonso M.J., *J. Control. Release.*, 2001, **73**, 255.

58. Calvo P., Remunan-Lopez., Vila-Jato J.L., Alonso M.J., *Pharm. Res.*, 1997, **14,** 1431.

59. Shah S., Pal A., Kaushik V.K., Devi S., *J. Appl. Polym. Sci. (Accepted).*

60. Sannan T., Kurita K., Ogura K., Iwakura Y., *Macromol. Chem.*, 1978, **19,** 458.

61. Rathke T.D., Hudson S.M., *J. Polym. Sci.*, 1993, **31**, 749.

62. Aiba S., *Int. J. Biol. Macromol.*, 1986, **8**, 173.

63. Muzzarelli R.A.A., Rochetti R., *Carbohydrate Polym.*, 1985, **5**, 461.

64. Terayama H., *J. Polym. Sci.*, 1952, **8**, 243.

65. Chen K.Q., Tongbao H., *J. Solid State Chem.*, 1990, **10**, 44.

66. Nanjo F., Katsumi R., Sakai K., *Anal. Biochem.*, 1991, **193**, 164.

67. Hiral A., Odani H., Nakajima A., *Polym. Bull.*, 1991, **26**, 87.

68. Curotto E., Aros F., *Anal. Biochem.*, 1993, **211**, 240.

69. Domard A., *Int. J. Biol. Macromol.*, 1987, **9**, 333.

70. Wu Y., Yang W., Wang C., Hu J., Fu S., *Int. J. Pharm.*, 2005, **295**, 235.

71. Hu Y., Lopina S.T., *J. Biomed. Mater. Res.*, 2005, **72**, 107.

72. Panyam J., Labhasetwar V., *Adv. Drug Deliv. Rev.*, 2003, ***55***, 329.

73. Gåserød O., Jolliffe A.G., Hampson F.C., Dettmar P.W.S., Kjak-Braek G., *Int. J. Pharm.*, 1998, **175**, 237.

74. Smith J., Wood E., Dornish M., *Pharm. Res.*, 2004, **21**, 43.

75. Panyam J., Zhou W. Z., Prabha S., Sahoo S.K. Labhasetwar V., *FASEB J.*, 2002, **16**, 1217.

76. Hu Y., Jiang X., Ding Y., Ge H., Yuan Y., Yang C., *Biomaterials.*, 2002, **23**, 319.

77. Kim S.S., Lee Y.M., *Macromer. Polym.*, 1995, **36**, 4497.

78. Quellec P., Gref R., Perrin L., Dellacherie E., Sommer F., Verbavatz J.M., *J. Biomed. Mater. Res.*, 1998, **42**, 45.

79. Hu B., Pan C., Sun Y., Hou Z., Ye H., Hu B., Zeng X., *J. Agric. Food Chem.*, Article in Press.

80. Ko J.A., Park H.J., Hmang S.J., Park J.B., Lee J.S., *Int. J Pharm.*, 1997, **37**, 152.

81. Singla A.K., Chawla M., *J Pharm. Pharmacol.*, 2001, **53**, 1047.

82. Wan Y, Creber K.A.M., Peppley B., Bui V.T., *Macromol.Chem.Phys.* 2003, **204**, 850.

83. Sarmento B., Ferreira D. Veiga D., Antonio Ribeiro., *Carbohydrate Polym.*, 2006, **66**, 1.

84. Ouchi T., Nishizawa H., Ohya Y., *Polymer.*, 1998, **39**, 5171.

85. Yu Y., Li W., Yu T., *Polym. Comm.*, 1991, **31**, 319.

86. Kaushik V.K and Bhardwaj A., *Polymer*, 1994, **13**, 355.

87. Kaushik V.K., *Polym. Test.*, 2000, **19**, 17

88. Klamerus K.J., Maloney K., Rudolph R. L., Sisenwine S.F., Jusko W.J., Chiang S.T., *J. Clin. Pharmacol.*, 1992, **32**, 716.

89. Burnett F.E., Dinan T.G., *Hum. Psychopharma.*, 1998, **13**, 169.

90. Yang H., Lopina S.T., *J. Biomed. Mater. Res.*, 2005, **72A**, 107.

91. Bajpai A.K., Bhanu S., *J. Macromol. Sci. Pure. & Appl. Chem.*, 2003, **40**, 265.

92. Gan Q., Wang T., *Colloids & Surf. B: Biointerfaces.*, 2007, **59**, 24.